

# Etaprime and Eta Mesons with Connection to Anomalous Glue

Steven D. Bass\*

*Kitzbühel Centre for Physics, Kitzbühel, Austria*

*Marian Smoluchowski Institute of Physics, Jagiellonian University, PL 30-348 Krakow, Poland*

Pawel Moskal†

*Marian Smoluchowski Institute of Physics, Jagiellonian University, PL 30-348 Krakow, Poland*

(Dated: 1 October 2018)

We review the present understanding of  $\eta'$  and  $\eta$  meson physics and these mesons as a probe of gluon dynamics in low-energy QCD. Recent highlights include the production mechanism of  $\eta$  and  $\eta'$  mesons in proton-nucleon collisions from threshold to high-energy, the  $\eta'$  effective mass shift in the nuclear medium, searches for possible  $\eta$  and  $\eta'$  bound states in nuclei as well as precision measurements of  $\eta$  decays as a probe of light-quark masses. We discuss recent experimental data, theoretical interpretation of the different measurements and the open questions and challenges for future investigation.

## CONTENTS

I. Introduction	1
II. QCD symmetries and the $\eta$ and $\eta'$	4
III. The strong CP problem and axions	9
IV. $\eta$ and $\eta'$ decays	9
A. Hadronic decays	10
B. Two-photon interactions	10
C. Precision tests of fundamental symmetries	12
V. $\eta$ - and $\eta'$ -nucleon interactions	12
A. The $N^*(1535)$ resonance and its structure	15
VI. The $\eta$ and $\eta'$ in nuclei	15
A. The $\eta'$ in medium	16
B. $\eta$ mesic nuclei	18
C. The $\eta'$ at finite temperature	19
VII. High-energy $\eta$ and $\eta'$ production	19
A. $\eta'$ - $\pi$ interactions and $1^{-+}$ exotics	20
VIII. Summary and Future Challenges	21
Acknowledgments	21
References	21

## I. INTRODUCTION

The  $\eta'$  meson is special in Quantum Chromodynamics, the theory of quarks and gluons (QCD), because of its strong affinity to gluons. Hadrons, their properties and interactions, are emergent from more fundamental QCD quark and gluon degrees of freedom. QCD has the property of asymptotic freedom. The coupling  $\alpha_s(P^2)$

which describes the strength of quark-gluon and gluon-gluon interactions decreases logarithmically with increasing (large) four-momentum transfer squared,  $P^2$ . In the infrared, at low  $P^2$ , quark-gluon interactions become strong. Quarks become confined inside hadron bound states and the vacuum is not empty but characterized by the formation of quark and gluon condensates. The physical degrees of freedom are emergent hadrons (protons, mesons ...) as bound states of quarks and gluons. Baryons like the proton are bound states of three valence quarks. Mesons are bound states of a quark and anti-quark.

Glue is manifest in the confinement potential which binds the quarks. This confinement potential corresponds to a restoring force of 10 tonnes regardless of separation. Quarks are bound by a string of glue which can break into two colorless hadron objects involving the creation of a quark-antiquark pair corresponding to the newly created ends of two confining strings formed from the original single string of confining glue. There are no isolated quarks. The QCD confinement radius is of order  $1\text{fm}=10^{-15}\text{m}$ . This physics at large coupling is beyond QCD perturbation theory and described either using QCD inspired models of hadrons which build in key symmetries of the underlying theory or through computational lattice methods. About 99% of the mass of the hydrogen atom, 938.8 MeV, is associated with the confinement potential with the masses of the electron 0.5 MeV and the proton 938.3 MeV. Inside the proton the masses of the proton's constituent two up quarks and one down quark are about 2.2 MeV for each up quark and 4.7 MeV for the down quark.

Besides generating the QCD confinement potential, glue plays a special role in the light hadron spectrum through the physics of the isoscalar  $\eta'$  and  $\eta$  mesons including their interactions. The QCD Lagrangian with massless quarks is symmetric between left- and right-

\* Steven.Bass@cern.ch

† P.Moskal@uj.edu.pl

handed quarks (which are fermions) or between positive and negative helicity quarks. However, this symmetry is missing in the ground state hadron spectrum. The lightest mass hadrons, pions and kaons, are pseudoscalar mesons called Goldstone bosons associated with the spontaneous breaking of chiral symmetry between left- and right-handed quarks. These mesons are special in that the square of their masses are proportional to the masses of their constituent valence quark-antiquark pair. (In contrast, the leading term in the masses of the proton and spin-one vector mesons is determined by the confining gluonic potential with contributions from the light quark masses treated as small perturbations.) The lightest mass pions, the neutral  $\pi^0$  with mass 135 MeV and charged  $\pi^\pm$  with mass 140 MeV, play an important role in nuclear physics and the nucleon-nucleon interaction. The isosinglet partners of the pions and kaons, the pseudoscalar  $\eta$  and  $\eta'$  mesons are too massive by about 300-400 MeV for them to be pure Goldstone states. They receive extra mass from non-perturbative gluon dynamics through a quantum effect called the axial anomaly. This glue comes with non-trivial topology. The physics of Goldstone bosons and the axial anomaly are explained in Section II below. Gluon topology is an effect beyond the simplest quark models and involves non-local and long range properties of the gluon fields. Theoretical understanding of the  $\eta$  and  $\eta'$  involves subtle interplay of local symmetries and non-local properties of QCD. Examples of topology in other branches of physics include the Bohm-Aharonov effect and topological phase transitions and phases of matter in condensed matter physics, the 2016 Nobel Prize for Physics.

The  $\eta$  and  $\eta'$  mesons come with rich phenomenology. The  $\eta'$  is predominantly a flavor-singlet state. This means that its wavefunction is approximately symmetric in the three lightest quark types (up, down and strange) that build up light hadron spectroscopy. These different species of quarks couple to gluons with equal strength. The  $\eta'$  meson has strong coupling to gluonic intermediate states in hadronic reactions from low through to high energies. An example from high energy reactions is the decay  $J/\Psi \rightarrow \eta'\gamma$ . The  $J/\Psi$  is made of a heavy charm-anticharm quark pair with mass 3686 MeV. Its decay to the light quark  $\eta'$  meson plus a photon involves the annihilation of the charm-anticharm quark pair into a gluonic intermediate state which then forms the  $\eta'$  meson made of a near symmetric superposition of light quark-antiquark pairs (up-antiup, down-antidown and strange-antistrange).

In this article we will discuss the broad spectrum of processes involving the  $\eta'$  that are mediated by gluonic intermediate states. The last 20 years has seen a dedicated programme of  $\eta'$  and  $\eta$  meson production experiments from nucleons and nuclei close to threshold as well as in high energy collisions. Studies of  $\eta$  and  $\eta'$  meson production and decay processes combine to teach

us about the interface of glue and chiral dynamics, the physics of Goldstone bosons, in QCD. Measurements of  $\eta$  and  $\eta'$  production in nuclear media are sensitive to behavior of fundamental QCD symmetries at finite density and temperature. In finite density nuclear media, for example in nuclei and neutron stars, hadrons propagate in the presence of long range mean fields that are created by nuclear many body dynamics. Interaction with the mean fields in the nucleus can change the hadrons' observed properties, *e.g.*, their effective masses, magnetic moments and axial charges. Symmetries between left- and right-handed quarks, which are spontaneously broken in the ground state, are partially restored in nuclear media with a reduced size of the quark condensate. At (large) finite temperature there is an effective renormalization of the QCD coupling which becomes reduced relative to the zero temperature theory for the same four-momentum transfer squared. One expects changes in hadron properties in the interaction region of finite temperature heavy-ion collisions. This article surveys  $\eta$  and  $\eta'$  meson physics as a probe of QCD dynamics emphasizing recent advances from experiments and theory.

In addition to the topics discussed here, the physics of glue in QCD features in many frontline areas of QCD hadron physics research. The planned electron-ion-collider (EIC) has an exciting programme to study the role of glue in nucleons and nuclei over a broad range of high energy kinematics (Accardi *et al.*, 2016; Deshpande, 2017). The search for hadrons containing explicit gluon degrees of freedom in their bound state wavefunctions is a hot topic in QCD spectroscopy, *e.g.*, possible glueball states built of two or three valence gluons and hybrids built of a quark-antiquark pair and a gluon (Klempt and Zaitsev, 2007). Gluons in the proton play an essential role in understanding the proton's internal spin structure (Aidala *et al.*, 2013). Studies of the QCD phase diagram (Braun-Munzinger and Wambach, 2009) from high density neutron stars (Lattimer and Prakash, 2016) to high temperature quark-gluon plasma and a color-glass condensate postulated to explain high density gluon matter in high energy collisions (Gyulassy and McLerran, 2005) are hot topics at the interface of nuclear and particle physics research. On the theoretical side, much effort is invested in trying to understand the detailed dynamics which leads to the QCD confinement potential (Greensite, 2011).

The plan of this paper is as follows.

In Section II we introduce the key theoretical issues with the  $\eta$  and  $\eta'$  mesons and their unique place at the interface of chiral and non-perturbative gluon dynamics. Here we explain the different gluonic effects at work in  $\eta$  and  $\eta'$  meson physics and how they are incorporated in theoretical calculations.

Section III discusses the strong CP puzzle. The observed matter antimatter asymmetry in the Universe requires some extra source of CP violation beyond

the quark mixing described by the Cabibbo-Kobayashi-Maskawa (CKM) matrix in the electroweak Standard Model. The non-perturbative glue which generates the large  $\eta'$  mass also has the potential to break CP symmetry in the strong interactions. This effect would be manifest as a finite neutron electric dipole moment proportional to a new QCD parameter,  $\theta_{\text{QCD}}$ , which is experimentally constrained to be very small, less than  $10^{-10}$ . One possible explanation for the absence of CP violation here involves a new light-mass pseudoscalar particle called the axion. The axion is also a possible dark matter candidate to explain the “missing mass” in the Universe. While no axion particle has so far been observed, these ideas have inspired a vigorous program of ongoing experimental investigation to look for them.

Sections IV-VII focus on  $\eta$  and  $\eta'$  phenomenology. In Section IV we discuss the information about QCD which follows from  $\eta$  and  $\eta'$  decay processes. The amplitude for the  $\eta$  meson to three pions decay depends on the difference between the lightest up and down quark masses and provides valuable information about the ratio of light quark masses. Studies of  $\eta$  and  $\eta'$  decays tell us about their internal quark-gluon and spatial structure. In addition, searches for rare decay processes provide valuable tests of fundamental symmetries.

Section V discusses  $\eta$  and  $\eta'$  production in near-threshold proton-nucleon collisions. The experimental program on  $\eta$  and  $\eta'$  nucleon interactions has focused on near-threshold meson production in proton-nucleon collisions and photoproduction from proton and deuteron targets (Krusche and Wilkin, 2014; Metag *et al.*, 2017; Moskal *et al.*, 2002; Wilkin, 2017). Recent highlights include the use of polarization observables in photoproduction experiments to search for new excited nucleon resonances (Anisovich *et al.*, 2017), measurement of the  $\eta'$  nucleon scattering length through the final state interaction in proton-proton collisions (Czerwinski *et al.*, 2014b) and measurement of the spin analyzing power to probe the partial waves associated with  $\eta$  production dynamics in proton-proton collisions (Adlarson *et al.*, 2018b).

Section VI deals with the  $\eta$  and  $\eta'$  in QCD nuclear media and the formation of possible meson-nucleus bound states. Recent photoproduction experiments in Bonn have revealed an  $\eta'$  effective mass shift in nuclear medium, which is about -40 MeV at nuclear matter density (Nanova *et al.*, 2013). Studies of the transparency of the nuclear medium to the propagating  $\eta'$  allow one to make a first (indirect) measurement of the  $\eta'$ -nucleus optical potential. One finds a small width of the  $\eta'$  in medium (Nanova *et al.*, 2012) compared to the depth of the optical potential meaning that the  $\eta'$  may be a good candidate for possible bound state searches in finite nuclei.

Mesic nuclei, if discovered in experiments, are a new exotic state of matter involving the meson being bound inside the nucleus purely by the strong interaction,

without electromagnetic Coulomb effects playing a role. Strong attractive interactions between the  $\eta$  meson and nucleons mean that both the  $\eta$  and  $\eta'$  are prime targets for mesic nuclei searches, with a vigorous ongoing program of experiments in both Europe and Japan (Metag *et al.*, 2017). Searches for possible  $\eta$  mesic nuclei are focused on helium while searches for  $\eta'$  bound states are focused on carbon and copper.

The  $\eta'$  effective mass shift in nuclei of about -40 MeV at nuclear matter density is in excellent agreement with the prediction of the Quark Meson Coupling model (Bass and Thomas, 2006) which works through coupling of the light up and down quarks in the meson to the  $\sigma$  (correlated two pion) mean field inside the nucleus. Here, the  $\eta'$  experiences an effective mass shift in nuclei which is catalyzed by its gluonic component (Bass and Thomas, 2014). Without this glue, the  $\eta'$  would be a strange quark state after SU(3) breaking with small interaction with the  $\sigma$  mean field inside the nucleus.

Shifting from finite density to finite temperature, there are also hints in data from RHIC (the Relativistic Heavy-Ion Collider) for possible  $\eta'$  mass suppression at finite temperature, with claims of at least -200 MeV mass shift (Csorgo *et al.*, 2010; Vertesi *et al.*, 2011).

Section VII discusses  $\eta$  and  $\eta'$  production in high-energy hadronic scattering processes from light-quark hadrons. The ratio of  $\eta$  to  $\pi$  meson production at high transverse momentum,  $p_t$ , in high-energy proton-nucleus and nucleus-nucleus collisions is observed to be independent of the target nucleus in relativistic heavy-ion collision data from RHIC at Brookhaven National Laboratory and the ALICE experiment at the Large Hadron Collider at CERN, indicating a common propagation through the nuclear medium in these kinematics. Interesting effects are also observed in high-energy  $\eta'$  production. The COMPASS experiment at CERN found that odd  $L$  exotic partial waves  $L^{-+}$  are strongly enhanced in  $\eta'\pi$  relative to  $\eta\pi$  exclusive production in collisions of 191 GeV negatively charged pions from hydrogen (Adolph *et al.*, 2015), consistent with expectations (Bass and Marco, 2002) based on gluon-mediated couplings of the  $\eta'$ .

In Section VIII we give conclusions and an outlook to possible future experiments which could shed new light on the structure and interactions of the  $\eta$  and  $\eta'$ .

Earlier reviews on  $\eta$  and  $\eta'$  meson physics, each with a different emphasis, are given in the volume edited by Bijmens *et al.* (2002). The lecture notes of Shore (2008) provide a theoretical overview of gluonic effects in  $\eta'$  physics. Axion physics is reviewed in Kawasaki and Nakayama (2013). Leutwyler (2013) discusses light-quark physics with focus on the  $\eta$  meson and Kupsc (2009) gives an overview of the analysis of  $\eta$  and  $\eta'$  meson decays. Meson production in proton-proton collisions close-to-threshold is discussed in detail in the reviews by Moskal *et al.* (2002), Krusche and Wilkin (2014) and Wilkin (2017). The present status of meson-nucleus interaction studies

is reviewed in Metag *et al.* (2017).

## II. QCD SYMMETRIES AND THE $\eta$ AND $\eta'$

Symmetries are important in hadron physics. Protons and neutrons with spin  $\frac{1}{2}$  are related through isospin SU(2), which is expanded to SU(3) to include  $\Sigma$  and  $\Lambda$  hyperons. Likewise, one finds SU(2) multiplets of spin-zero and spin-one mesons, *e.g.*, the charged and neutral spin-zero pions are isospin partners and reside inside SU(3) multiplets together with kaons. This spectroscopy suggests that these hadronic particles are built from simpler constituents. These are spin  $\frac{1}{2}$  quarks labeled up, down and strange (their flavor denoted  $u$ ,  $d$  and  $s$ ). These quarks carry electric charges  $e_u = +\frac{2}{3}$  and  $e_d, e_s = -\frac{1}{3}$  where, *e.g.*, a proton is built from two up quarks and a down quark, and a neutron is built of two down quarks and an up quark. The spin-zero and spin-one mesons are built of a quark-antiquark combination. The hadron wavefunctions are symmetric in flavor-spin and spatial degrees of freedom. The Pauli principle is ensured with the quarks and antiquarks being antisymmetric in a new label called color SU(3), red, green and blue.

High energy deep inelastic scattering experiments probe the deep structure of hadrons by scattering high energy electron or muon beams off hadronic targets. Deeply virtual photon exchange acts like a microscope which allows us to look deep inside the proton. One measures the inclusive cross section. These experiments reveal a proton built of nearly free fermion constituents, called partons.

The deep inelastic results and spectroscopy come together when color is made dynamical in the theory of Quantum Chromodynamics, QCD. Quarks carry a color charge and interact through colored gluon exchange, like electrons interacting through photon exchange in Quantum Electrodynamics, QED. QCD differs from QED in that gluons also carry color charge whereas photons are electrically neutral. (The dynamics is governed by the gauge group of color SU(3) instead of U(1) for the photon.) This means that the Feynman diagrams for QCD include 3 gluon and 4 gluon vertices (as well as the quark gluon vertices) and that gluons self-interact. For excellent textbook discussions of QCD and its application to hadrons see Close (1979) and Thomas and Weise (2001).

Gluon-gluon interactions induce asymptotic freedom: the QCD version of the fine structure constant for quark-gluon and gluon-gluon interactions,  $\alpha_s$ , decreases logarithmically with increasing resolution  $Q^2$ . Gluon bremsstrahlung results in gluon induced jets of hadronic particles which were first discovered in high energy  $e^-e^+$  collisions at DESY (Ellis, 2014). Quark and gluon partons play a vital role in high energy hadronic collisions, *e.g.*, at the Large Hadron Collider at CERN (Altarelli, 2013). Deep inelastic scattering experiments also tell us

that about 50% of the proton's momentum perceived at high  $Q^2$  is carried by gluons, consistent with the QCD prediction for the deepest structure of the proton. QCD theory also predicts that about 50% of the proton's angular momentum budget is contributed by gluon spin and orbital angular momentum (Aidala *et al.*, 2013; Bass, 2005).

Glue in low energy QCD is manifest through the confinement potential which binds quarks inside hadrons. Color-singlet glueball excitations (bound states of gluons) as well as hybrid bound states of a quark and anti-quark plus gluon are predicted by theory but still awaiting decisive experimental confirmation.

The decay amplitude for  $\pi^0 \rightarrow 2\gamma$  and the ratio of cross-sections for hadron to muon-pair production in high energy electron-positron collisions,  $R_{e^+e^-}$ , are proportional to the number of dynamical colors  $N_c$ , giving an experimental confirmation of  $N_c = 3$ .

This dynamics is encoded in the QCD Lagrangian. We first write the quark field  $\psi$  as the sum of left- and right-handed quark components  $\psi = \psi_L + \psi_R$  where  $\psi_L = \frac{1}{2}(1 - \gamma_5)\psi$  and  $\psi_R = \frac{1}{2}(1 + \gamma_5)\psi$  project out different states of quark helicity. The vector gluon field is denoted  $A_\mu^b$ . For massless quarks, the QCD Lagrangian reads

$$\mathcal{L}_{\text{QCD}} = \bar{\psi}_L i\gamma^\mu D_\mu \psi_L + \bar{\psi}_R i\gamma^\mu D_\mu \psi_R - \frac{1}{2} \text{Tr} G^{\mu\nu} G_{\mu\nu}. \quad (1)$$

Here  $D_\mu \psi = (\partial_\mu - igA_\mu)\psi$  describes the quark-gluon interaction;  $G^{\mu\nu} = \partial^\mu A^\nu - \partial^\nu A^\mu + gf_{abc}A_b^\mu A_c^\nu$  is the gluon field tensor with the last term here generating the 3-gluon and 4-gluon interactions. The quark-gluon dynamics is determined by requiring invariance under the gauge transformations

$$\begin{aligned} \psi &\rightarrow \mathcal{G}\psi \\ A_\mu &\rightarrow \mathcal{G}A_\mu\mathcal{G}^{-1} + \frac{i}{g}(\partial_\mu\mathcal{G})\mathcal{G}^{-1} \end{aligned} \quad (2)$$

where  $\mathcal{G}$  describes rotating the local color phase of the quark fields.

For massless quarks the left- and right- handed quarks transform independently under chiral rotations which rotate between up, down and strange flavored quarks. Finite quark masses through the Lagrangian term  $m\bar{\psi}\psi$  explicitly breaks the chiral symmetry by connecting left- and right-handed quarks,

$$\bar{\psi}\psi = \bar{\psi}_L\psi_R + \bar{\psi}_R\psi_L. \quad (3)$$

Quark chirality (-1 for a left-handed quark and +1 for a right-handed quark) and helicity are conserved in perturbative QCD with massless quarks.

Low energy QCD is characterized by confinement and dynamical chiral symmetry breaking. There is an absence of parity doublets in the light-hadron spectrum. For example, the  $J^P = \frac{1}{2}^+$  proton and the lowest mass

$J^P = \frac{1}{2}^-$  N\*(1535) nucleon resonance (that one would normally take as chiral partners) are separated in mass by 597 MeV. This tells us that the chiral symmetry for light  $u$  and  $d$  (and  $s$ ) quarks is spontaneously broken.

Spontaneous symmetry breaking means that the symmetry of the Lagrangian is broken in the vacuum. One finds a non-vanishing chiral condensate connecting left- and right-handed quarks

$$\langle \text{vac} | \bar{\psi}\psi | \text{vac} \rangle < 0. \quad (4)$$

This spontaneous symmetry breaking induces an octet of light-mass pseudoscalar Goldstone bosons associated with SU(3) including the pions and kaons which are listed in Table I and also – see below – (before extra gluonic effects in the singlet channel) a flavor-singlet Goldstone state.<sup>1</sup>

The Goldstone bosons  $P$  couple to the axial-vector currents which play the role of Noether currents through

$$\langle \text{vac} | J_{\mu 5}^i | P(p) \rangle = -i f_P^i p_\mu e^{-ip \cdot x} \quad (5)$$

with  $f_P^i$  the corresponding decay constants (which determine the strength for, *e.g.*,  $\pi^- \rightarrow \mu^- \bar{\nu}_\mu$ ) and satisfy the Gell-Mann-Oakes-Renner (GMOR) relation (Gell-Mann *et al.*, 1968)

$$m_P^2 f_P^2 = -m_q \langle \bar{\psi}\psi \rangle + \mathcal{O}(m_q^2) \quad (6)$$

with  $f_\pi = \sqrt{2} F_\pi = 131$  MeV. The mass squared of the Goldstone bosons  $m_P^2$  is in first order proportional to the mass of their valence quarks, Eqs. (5,6). This picture is the starting point of successful pion and kaon phenomenology.

A scalar confinement potential implies dynamical chiral symmetry breaking. For example, in the Bag model of quark confinement is modeled by an infinite square well scalar potential. When quarks collide with the Bag wall, their helicity is flipped. The Bag wall thus connects left and right handed quarks leading to quark-pion coupling and the pion cloud of the nucleon (Thomas, 1984). Quark-pion coupling connected to chiral symmetry plays an important role in the proton's dynamics and phenomenology, *e.g.*, transferring net quark spin into pion cloud orbital angular momentum and thus playing an important role in the nucleon's spin structure (Bass and Thomas, 2010).

The light mass pion is especially important in nuclear physics, also with strong coupling to the lightest mass  $\Delta$  p-wave nucleon resonance.

The QCD Hamiltonian is linear in the quark masses. For small quark masses this allows one to perform a rigorous expansion perturbing in  $m_q \propto m_\pi^2$ , called the chiral expansion (Gasser and Leutwyler, 1982). The proton mass in the chiral limit of massless quarks is determined by gluonic binding energy and set by  $\Lambda_{\text{QCD}}$ , which sets the scale for the running of the QCD coupling  $\alpha_s$ ,  $\Lambda_{\text{QCD}} = 332 \pm 17$  MeV for QCD with 3 flavors (Patrignani *et al.*, 2016).

The lightest up and down quark masses are determined from detailed studies of chiral dynamics. One finds  $m_u = 2.2_{-0.4}^{+0.6}$  MeV and  $m_d = 4.7_{-0.3}^{+0.5}$  MeV whereas the strange quark mass is slightly heavier at  $m_s = 95 \pm 5$  MeV (with all values here quoted at the scale  $\mu = 2$  GeV according to the Particle Data Group (Patrignani *et al.*, 2016)).

When electromagnetic interactions are also included, the leading order mass relations (6) become (Georgi, 1984)

$$\begin{aligned} m_{\pi^\pm}^2 &= \mu(m_u + m_d) + \Delta m^2 \\ m_{K^\pm}^2 &= \mu(m_u + m_s) + \Delta m^2 \\ m_{K^0}^2 &= \mu(m_d + m_s) \\ m_{\pi^0}^2 &= \mu(m_u + m_d) \\ m_{\eta_8}^2 &= \mu(4m_s + m_u + m_d) \end{aligned} \quad (7)$$

where  $\Delta m^2$  is the electromagnetic contribution (Dashen, 1969) and  $\mu = -\langle \bar{\psi}\psi \rangle / f_\pi^2$ . Substituting the pion and kaon masses gives the leading-order quark mass ratios

$$\left. \frac{m_s}{m_d} \right|_{\text{LO}} = 20, \quad \left. \frac{m_u}{m_d} \right|_{\text{LO}} = 0.55. \quad (8)$$

The leading order GMOR formula, Eq. (6), gives the Gell-Mann Okubo formula (Gell-Mann, 1961; Okubo, 1962) for the octet state

$$4m_K^2 - m_\pi^2 = 3m_{\eta_8}^2. \quad (9)$$

Numerically  $m_\eta(548\text{MeV}) \simeq m_{\eta_8}(570\text{MeV})$ . The  $\eta$  meson mass and this  $\eta_8$  mass contribution agree within 4% accuracy.

TABLE I The octet of Goldstone bosons corresponding to chiral SU(3) and their masses in free space.

Meson	wavefunction	mass (MeV)
$\pi^0$	$\frac{1}{\sqrt{2}}(u\bar{u} - d\bar{d})$	135
$\pi^+$	$u\bar{d}$	140
$\pi^-$	$\bar{u}d$	140
$K^0$	$d\bar{s}$	498
$\bar{K}^0$	$s\bar{d}$	498
$K^+$	$u\bar{s}$	494
$K^-$	$\bar{u}s$	494
$\eta_8$	$\frac{1}{\sqrt{6}}(u\bar{u} + d\bar{d} - 2s\bar{s})$	$\frac{4}{3}m_K^2 - \frac{1}{3}m_\pi^2$

<sup>1</sup> Goldstone's theorem tells us that there is one massless pseudoscalar boson for each symmetry generator that does not annihilate the vacuum.

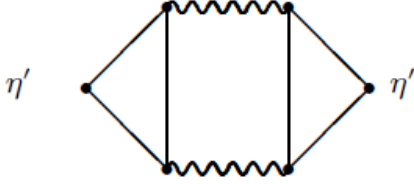


FIG. 1 Gluonic intermediate states contribute to the  $\eta'$ . The  $\eta'$  mixes a chirality-two quark-antiquark contribution and chirality-zero gluonic contribution.

However, this is not the full story. The quark condensate in Eq. (6) also spontaneously breaks axial U(1) symmetry meaning that one might also expect a flavor-singlet Goldstone state which mixes with the octet state to generate the isosinglet bosons. However, without extra input, the resultant bosons do not correspond to states in the physical spectrum. The lightest mass isosinglet bosons, the  $\eta$  and  $\eta'$ , are about 300-400 MeV too heavy to be pure Goldstone states, with masses  $m_\eta = 548$  MeV and  $m_{\eta'} = 958$  MeV. One needs extra mass in the flavor-singlet channel to connect to the physical  $\eta$  and  $\eta'$  mesons. This mass is associated with non-perturbative gluon dynamics.

The flavor-singlet channel is sensitive to processes involving violation of the Okubo-Zweig-Iizuka (OZI) rule, where the quark-antiquark pair (with quark chirality equal two) propagates with coupling to gluonic intermediate states (with zero net chirality); see Fig. 1. The OZI rule (Iizuka, 1966; Okubo, 1963; Zweig, 1964) is the phenomenological observation that hadronic processes involving Feynman graphs mediated by gluons (without continuous quark lines connecting the initial and final states) tend to be strongly suppressed.

To see the effect of the gluonic mass contribution consider the  $\eta$ - $\eta'$  mass matrix for free mesons with rows and columns in the octet-singlet basis

$$\eta_8 = \frac{1}{\sqrt{6}} (u\bar{u} + d\bar{d} - 2s\bar{s}), \quad \eta_0 = \frac{1}{\sqrt{3}} (u\bar{u} + d\bar{d} + s\bar{s}). \quad (10)$$

At leading order in the chiral expansion (taking terms proportional to the quark masses  $m_q$ ) this reads

$$M^2 = \begin{pmatrix} \frac{4}{3}m_K^2 - \frac{1}{3}m_\pi^2 & -\frac{2}{3}\sqrt{2}(m_K^2 - m_\pi^2) \\ -\frac{2}{3}\sqrt{2}(m_K^2 - m_\pi^2) & [\frac{2}{3}m_K^2 + \frac{1}{3}m_\pi^2 + \tilde{m}_{\eta_0}^2] \end{pmatrix}. \quad (11)$$

Here  $\tilde{m}_{\eta_0}^2$  is the flavor-singlet gluonic mass term.

In the notation of Eq.(7) these singlet and mixing terms are

$$\begin{aligned} m_{8,0}^2 &= \mu(m_u + m_d - 2m_s), \\ m_0^2 &= \mu(m_u + m_d + m_s) + \tilde{m}_{\eta_0}^2. \end{aligned} \quad (12)$$

The masses of the physical  $\eta$  and  $\eta'$  mesons are found

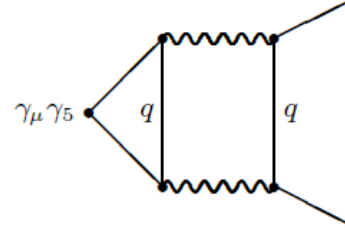


FIG. 2 Coupling of the axial-vector current through gluonic intermediate states. Gluon propagators are shown as wavy lines. Straight lines denote quark propagators.

by diagonalizing this matrix, *viz.*

$$\begin{aligned} |\eta\rangle &= \cos\theta |\eta_8\rangle - \sin\theta |\eta_0\rangle \\ |\eta'\rangle &= \sin\theta |\eta_8\rangle + \cos\theta |\eta_0\rangle \end{aligned} \quad (13)$$

One obtains values for the  $\eta$  and  $\eta'$  masses:

$$\begin{aligned} m_{\eta',\eta}^2 &= (m_K^2 + \tilde{m}_{\eta_0}^2/2) \\ &\pm \frac{1}{2} \sqrt{(2m_K^2 - 2m_\pi^2 - \frac{1}{3}\tilde{m}_{\eta_0}^2)^2 + \frac{8}{9}\tilde{m}_{\eta_0}^4}. \end{aligned} \quad (14)$$

Here the lightest mass state is the  $\eta$  and heavier state is the  $\eta'$ . Summing over the two eigenvalues in Eq.(14) gives the Witten-Veneziano mass formula (Veneziano, 1979; Witten, 1979a)

$$m_\eta^2 + m_{\eta'}^2 = 2m_K^2 + \tilde{m}_{\eta_0}^2. \quad (15)$$

The gluonic mass term is obtained by substituting the physical values of  $m_\eta$ ,  $m_{\eta'}$  and  $m_K$  to give  $\tilde{m}_{\eta_0}^2 = 0.73\text{GeV}^2$ . Without the gluonic mass term the  $\eta$  would be approximately an isosinglet light-quark state ( $\frac{1}{\sqrt{2}}|\bar{u}u + \bar{d}d\rangle$ ) with mass  $m_\eta \sim m_\pi$  degenerate with the pion and the  $\eta'$  would be a strange-quark state  $|\bar{s}s\rangle$  with mass  $m_{\eta'} \sim \sqrt{2m_K^2 - m_\pi^2}$  — mirroring the isoscalar vector  $\omega$  and  $\phi$  mesons.

When interpreted in terms of the leading order mixing scheme, Eq. (13), phenomenological studies of various decay processes give a value for the  $\eta$ - $\eta'$  mixing angle between  $-15^\circ$  and  $-20^\circ$  (Ambrosino *et al.*, 2009; Ball *et al.*, 1996; Gilman and Kauffman, 1987). The  $\eta'$  has a large flavor-singlet component with strong affinity to couple to gluonic degrees of freedom. Mixing means that non-perturbative glue through axial U(1) dynamics plays an important role in both the  $\eta$  and  $\eta'$  and their interactions.

The gluonic mass term is associated with the QCD axial anomaly in the divergence of the flavor-singlet axial-vector current. While the non-singlet axial-vector currents are partially conserved (they have just mass terms in the divergence), the singlet current  $J_{\mu 5} = \bar{u}\gamma_\mu\gamma_5 u + \bar{d}\gamma_\mu\gamma_5 d + \bar{s}\gamma_\mu\gamma_5 s$  satisfies the divergence equation (Adler, 1969; Bell and Jackiw, 1969)

$$\partial^\mu J_{\mu 5} = 6Q + \sum_{k=1}^3 2im_k \bar{q}_k \gamma_5 q_k \quad (16)$$

where  $Q = \frac{\alpha_s}{8\pi} G_{\mu\nu} \tilde{G}^{\mu\nu}$  is called the topological charge density. The anomalous gluonic term  $Q$  is induced by QCD quantum effects associated with renormalization of the singlet axial-vector current <sup>2</sup>. Here  $G_{\mu\nu}$  is the gluon field tensor and  $\tilde{G}^{\mu\nu} = \frac{1}{2}\epsilon^{\mu\nu\alpha\beta}G_{\alpha\beta}$ . For reviews of anomaly physics see Shifman (1991) and Ioffe (2006). Since gluons couple equally to each flavor of quark the anomaly term cancels in the divergence equations for non-singlet currents like  $J_{\mu 5}^{(3)} = \bar{u}\gamma_\mu\gamma_5 u - \bar{d}\gamma_\mu\gamma_5 d$  and  $J_{\mu 5}^{(8)} = \bar{u}\gamma_\mu\gamma_5 u + \bar{d}\gamma_\mu\gamma_5 d - 2\bar{s}\gamma_\mu\gamma_5 s$ .

The QCD anomaly means that the singlet current  $J_{\mu 5}$  is not conserved for massless quarks. Non-perturbative gluon processes act to connect left- and right-handed quarks, whereas left- and right-handed massless quarks propagate independently in perturbative QCD with helicity conserved for massless quarks.

The integral over space  $\int d^4z Q = n$  is quantized with either integer or fractional values and measures a property called the topological winding number. This winding number vanishes in perturbative QCD and in QED but is finite with non-perturbative glue, *e.g.*, it is an integer for instantons (tunneling processes in the QCD vacuum that flip quark chirality) (Crewther, 1978) <sup>3</sup>. The gluonic mass term is generated by glue associated with this non-trivial topology, related perhaps to confinement or to instantons (Fritzsche and Minkowski, 1975; 't Hooft, 1976a,b; Kogut and Susskind, 1975; Witten, 1979b). The exact details of this gluon dynamics are still debated.

It is interesting to consider QCD in the limit of a large number of colors,  $N_c \rightarrow \infty$ . There are two well defined theoretical limits taking  $\alpha_s N_c$  and either  $N_f$  (the number of flavors) or  $N_f/N_c$  held fixed. The gluonic mass term has a rigorous interpretation as the leading term when one makes an expansion in  $1/N_c$  in terms of a quantity  $\chi(0)$  called the Yang-Mills topological susceptibility,

$$\tilde{m}_{\eta_0}^2 \Big|_{\text{LO}} = -\frac{6}{f_\pi^2} \chi(0) \Big|_{\text{YM}} \quad (17)$$

<sup>2</sup> In QCD the flavor-singlet axial-vector current can couple through gluon intermediate states; see Fig. 2. Here the triangle Feynman diagram is essential with the axial-vector current  $\gamma_\mu\gamma_5$  and two gluon couplings  $\gamma_\alpha$  and  $\gamma_\beta$  as the three vertices. When we regularize the ultraviolet behavior of momenta in the triangle loop, we find that we can preserve current conservation at the quark-gluon-vertices (necessary for gauge invariance) or partial conservation of the axial-vector current but not both simultaneously. Current conservation wins and induces the gluonic anomaly term in the singlet divergence equation, Eq.(16), from the ultraviolet point-like part of the triangle loop.

<sup>3</sup> For a gluon field  $A_\mu$  with gauge transformation  $\mathcal{G}$ ,  $A_\mu \rightarrow \mathcal{G}^{-1}A_\mu\mathcal{G} + \frac{1}{g}\mathcal{G}^{-1}(\partial_\mu\mathcal{G})$ . Finite action requires that  $A_\mu$  should tend to a pure gauge configuration when  $x \rightarrow \infty$  with finite surface term integral  $\int d^4x Q$  which takes quantized values, the topological winding number.

– for extended discussion see Shore (1998, 2008). Here

$$\chi(k^2)|_{\text{YM}} = \int d^4z i e^{ik \cdot z} \langle \text{vac} | T Q(z)Q(0) | \text{vac} \rangle \Big|_{\text{YM}} \quad (18)$$

is calculated in the pure glue theory (without quarks). If we assume that the topological winding number remains finite independent of the value of  $N_c$  then  $\tilde{m}_{\eta_0}^2 \sim 1/F_\pi^2 \sim 1/N_c$  as  $N_c \rightarrow \infty$  (Witten, 1979a). In recent computational QCD lattice calculations Cichy *et al.* (2015) have computed both the pure gluonic term on the right-hand side of Eq.(18) and the meson mass contributions with dynamical quarks in the Witten-Veneziano formula Eq.(15) and find excellent agreement at the 10% percent level. This calculation gives  $\chi^{1/4}(0)|_{\text{YM}} = 185.3 \pm 5.6$  MeV, very close to the phenomenological value 180 MeV which follows from taking  $\tilde{m}_{\eta_0}^2 = 0.73\text{GeV}^2$  in the Witten-Veneziano formula Eq.(15).

Independent of the detailed QCD dynamics one can construct low-energy effective chiral Lagrangians which include the effect of the anomaly and axial U(1) symmetry (Di Vecchia and Veneziano, 1980; Kawarabayashi and Ohta, 1980; Leutwyler, 1998; Nath and Arnowitt, 1981; Rosenzweig *et al.*, 1980; Witten, 1980) and use these Lagrangians to study low-energy processes involving the  $\eta$  and  $\eta'$ . We define  $U = e^{i(\phi/F_\pi + \sqrt{\frac{2}{3}}\eta_0/F_0)}$  as the unitary meson matrix where  $\phi = \sum \pi_a \lambda_a$  denotes the octet of would-be Goldstone bosons  $\pi_a$  associated with spontaneous chiral symmetry breaking with  $\lambda_a$  the Gell-Mann matrices (SU(3) generalisations of the isospin SU(2) Pauli matrices that couple to pions),  $\eta_0$  is the singlet boson and  $F_0$  is the singlet decay constant (at leading order taken to be equal to  $F_\pi=92$  MeV). With this notation the kinetic energy and mass terms in the chiral Lagrangian are

$$\mathcal{L} = \frac{F_\pi^2}{4} \text{Tr}(\partial^\mu U \partial_\mu U^\dagger) + \frac{F_\pi^2}{4} \text{Tr} M \left( U + U^\dagger \right) \quad (19)$$

with  $M$  the meson mass matrix. The gluonic mass term  $\tilde{m}_{\eta_0}^2$  is introduced via a flavor-singlet potential involving the topological charge density  $Q$  which is constructed so that the Lagrangian also reproduces the axial anomaly. This potential reads

$$\frac{1}{2} i Q \text{Tr} \left[ \log U - \log U^\dagger \right] + \frac{3}{\tilde{m}_{\eta_0}^2 F_0^2} Q^2 \mapsto -\frac{1}{2} \tilde{m}_{\eta_0}^2 \eta_0^2 \quad (20)$$

where  $Q$  is eliminated through its equation of motion to give the gluonic mass term for the  $\eta'$ . The Lagrangian contains no kinetic energy term for  $Q$ , meaning that the gluonic potential does not correspond to a physical state;  $Q$  is therefore distinct from mixing with a pseudoscalar glueball state. The  $Q\eta_0$  coupling in Eq.(20) reproduces the picture of the  $\eta'$  as a mixture of chirality  $\pm 2$  quark-antiquark and chirality-zero gluonic contributions; see Fig. 1.

Higher-order terms in  $Q^2$  become important when we consider scattering processes involving more than one  $\eta'$  or  $\eta$  (Di Vecchia *et al.*, 1981), *e.g.*, the term  $Q^2 \partial_\mu \pi_a \partial^\mu \pi_a$  gives an OZI-violating tree-level contribution to the decay  $\eta' \rightarrow \eta \pi \pi$ . For the  $\eta'$  in a nuclear medium at finite density, the medium dependence of  $\tilde{m}_{\eta_0}^2$  may be introduced through coupling to the  $\sigma$  mean field in the nucleus through the interaction term  $\mathcal{L}_{\sigma Q} = g_{\sigma Q} Q^2 \sigma$ . Here  $g_{\sigma Q}$  denotes coupling to the  $\sigma$  field. Again eliminating  $Q$  through its equation of motion, one finds the gluonic mass term decreases in-medium  $\tilde{m}_{\eta_0}^{*2} < \tilde{m}_{\eta_0}^2$  independent of the sign of  $g_{\sigma Q}$  and the medium acts to partially neutralize axial U(1) symmetry breaking by gluonic effects (Bass and Thomas, 2006). We return to this physics in Section VI below. In general, couplings involving  $Q$  give OZI-violation in physical observables.

Recent QCD lattice calculations suggest (partial) restoration of axial U(1) symmetry at finite temperature (Bazavov *et al.*, 2012; Cossu *et al.*, 2013; Tomiya *et al.*, 2017).

There are several places that glue enters  $\eta'$  and  $\eta$  meson physics: the gluon topology potential which generates the large  $\eta'$  mass, possible small mixing with a lightest mass pseudoscalar glueball state (which comes with a kinetic energy term in its Lagrangian) and, in high momentum transfer processes, radiatively generated glue associated with perturbative QCD. Possible candidates for the pseudoscalar glueball state are predicted by lattice QCD calculations with a mass above 2 GeV (Gregory *et al.*, 2012a; Morningstar and Peardon, 1999; Sun *et al.*, 2017). These different gluonic contributions are distinct physics.

We have so far discussed the  $\eta$  and  $\eta'$  at leading order in the chiral expansion. Going beyond leading order, one becomes sensitive to extra SU(3) breaking through the difference in the pion and kaon decay constants,  $F_K = 1.22 F_\pi$ , as well as new OZI-violating couplings. One finds strong mixing also in the decay constants. Two mixing angles enter the  $\eta - \eta'$  system when one extends the theory to  $O(p^4)$  in the meson momentum (Leutwyler, 1998), *viz.*

$$\begin{aligned} f_\eta^8 &= f_8 \cos \theta_8, & f_{\eta'}^8 &= f_8 \sin \theta_8 \\ f_\eta^0 &= -f_0 \sin \theta_0, & f_{\eta'}^0 &= f_0 \cos \theta_0. \end{aligned} \quad (21)$$

These mixing angles follow because the eigenstates of the mass matrix involve linear combinations of the different decay constants separated by SU(3) breaking multiplying the meson states. In the SU(3) symmetric world  $F_\pi = F_K$  one would have  $\theta_8 = \theta_0$ , with both vanishing for massless quarks. One finds a systematic expansion, large  $N_c$  chiral perturbation theory, in  $1/N_c = O(\delta)$ ,  $p = O(\sqrt{\delta})$  and  $m_q = O(\delta)$ , where  $m_q$  are the light quark masses and  $\tilde{m}_{\eta_0}^2 \sim 1/N_c$ .

Phenomenological fits have been made to production and decay processes within this two mixing angle scheme.

Best fit values quoted in Feldmann (2000) are

$$\begin{aligned} f_8 &= (1.26 \pm 0.04) f_\pi, & \theta_8 &= -21.2^\circ \pm 1.6^\circ \\ f_0 &= (1.17 \pm 0.03) f_\pi, & \theta_0 &= -9.2^\circ \pm 1.7^\circ \end{aligned} \quad (22)$$

with the fits assuming that any extra OZI-violation beyond  $\tilde{m}_{\eta_0}^2$  can be turned off in first approximation. Similar numbers are obtained in Escribano and Frere (2005) and Shore (2006) and in recent QCD lattice calculations (Bali *et al.*, 2018; Ottnad and Urbach, 2018). To good approximation, this scheme reduces to one mixing angle if we change to the quark flavor basis  $\frac{1}{\sqrt{2}}(u\bar{u} + d\bar{d})$  and  $s\bar{s}$ , *viz.*  $\phi = 39.3^\circ \pm 1^\circ$  (Feldmann, 2000). These numbers correspond to a mixing angle about  $-15^\circ$  in the leading order formula Eq.(13) (Feldmann *et al.*, 1998).

Recent QCD lattice calculations give values for the mixing angles:  $34 \pm 3^\circ$  (Gregory *et al.*, 2012b) and  $46 \pm 1 \pm 3^\circ$  (Michael *et al.*, 2013; Urbach, 2017) in the quark flavor basis and  $-14.1 \pm 2.8^\circ$  in the (leading order) octet-singlet basis (Christ *et al.*, 2010).

Before discussing phenomenology, we first mention two key issues connected to the QCD anomaly which need to be kept in mind when understanding the  $\eta'$ . Observables do not depend on renormalization scales and are gauge invariant; that is, they do not depend on how a theoretician has set up a calculation.

First, the current  $J_{\mu 5}$  picks up a dependence on the renormalization scale through the two-loop Feynman diagram in Fig. 2 (Crewther, 1978; Kodaira, 1980). This means that the singlet decay constant  $F_0$  in QCD is sensitive to renormalization scale dependence. This is in contrast to  $F_\pi$  which is measured by the anomaly-free current  $J_{\mu 5}^{(3)}$ . A renormalization group (RG) scale invariant version of  $F_0$  suitable for phenomenology can be defined by factoring out the scale dependence or, equivalently, taking the RG scale dependent quantity evaluated at  $\mu^2 = \infty$ . Numerically, the RG factor is about 0.84 if we take  $\alpha_s(\mu_0^2) \sim 0.6$  as typical of the infrared region of QCD and evolve to infinity working to  $O(\alpha_s^2)$  in perturbative QCD (Bass, 2005).

Second, the topological charge density is a total divergence  $Q = \partial^\mu K_\mu$ . Here  $K_\mu$  is the anomalous Chern-Simons current

$$K_\mu = \frac{g^2}{32\pi^2} \epsilon_{\mu\nu\rho\sigma} \left[ A_a^\nu \left( \partial^\rho A_a^\sigma - \frac{1}{3} g f_{abc} A_b^\rho A_c^\sigma \right) \right] \quad (23)$$

with  $A_a^\mu$  the gluon field and  $\alpha_s = g^2/4\pi$  is the QCD coupling. The current  $K_\mu$  is gauge dependent. Gauge dependence issues arise immediately if one tries to separate a “ $K_\mu$  contribution” from matrix elements of the singlet current  $J_{\mu 5}$ . This means that isolating the gluonic leading Fock component from the  $\eta'$  involves subtle issues of gauge invariance and only makes sense with respect to a particular renormalization scheme like the gauge invariant scheme  $\overline{\text{MS}}$  (Bass, 2009).



### III. THE STRONG CP PROBLEM AND AXIONS

The gluonic topology term (20) which generates the gluonic contribution to the  $\eta'$  mass also has the potential to induce strong CP violation in QCD. One finds an extra term,  $-\theta_{\text{QCD}}Q$ , in the effective Lagrangian for axial U(1) physics which ensures that the potential

$$\frac{1}{2}iQ\text{Tr}\left[\log U - \log U^\dagger\right] + \frac{3}{\tilde{m}_{\eta_0}^2 F_0^2}Q^2 - \theta_{\text{QCD}}Q \quad (24)$$

is invariant under axial U(1) transformations with  $U \rightarrow e^{-2i\alpha}U$  acting on the quark fields being compensated by  $\theta_{\text{QCD}} \rightarrow \theta_{\text{QCD}} - 2\alpha N_f$ .

The term  $\theta_{\text{QCD}}Q$  is odd under CP symmetry. If it has non-zero value,  $\theta_{\text{QCD}}$  induces a non zero neutron electric dipole moment (Crewther *et al.*, 1979)

$$d_n = 5.2 \times 10^{-16} \theta_{\text{QCD}} \text{ ecm}. \quad (25)$$

Experiments constrain  $|d_n| < 3.0 \times 10^{-26} \text{ e.cm}$  at 90% confidence limit or  $\theta_{\text{QCD}} < 10^{-10}$  (Pendlebury *et al.*, 2015). New and ongoing experiments aim for an order of magnitude improvement in precision within the next five years or so (Schmidt-Wellenburg, 2016).

Why is the strong CP violation parameter  $\theta_{\text{QCD}}$  so small? QCD alone offers no answer to this question. QCD symmetries allow for a possible  $\theta_{\text{QCD}}$  term but do not constrain its size. The value of  $\theta_{\text{QCD}}$  is an external parameter in the theory just like the quark masses are.

Non-perturbative QCD arguments tell us that if the lightest quark had zero mass, then there would be no net CP violation connected to the  $\theta_{\text{QCD}}$  term (Weinberg, 1996). However, chiral dynamics including the  $\eta \rightarrow 3\pi$  decay discussed below tells us that the lightest up and down flavor quarks have small but finite masses. In the full Standard Model the parameter which determines the size of strong CP violation is  $\Theta_{\text{QCD}} = \theta_{\text{QCD}} + \text{Arg det } \mathcal{M}_q$ , where  $\mathcal{M}_q$  is the quark mass matrix. Possible strong CP violation then links QCD and the Higgs sector in the Standard Model that determines the quark masses.

A possible resolution of this strong CP puzzle is to postulate the existence of a new very-light mass pseudoscalar called the axion (Weinberg, 1978; Wilczek, 1978) which couples through the Lagrangian term

$$\begin{aligned} \mathcal{L}_a = & -\frac{1}{2}\partial_\mu a \partial^\mu a + \left[\frac{a}{M} - \Theta_{\text{QCD}}\right] \frac{\alpha_s}{8\pi} G_{\mu\nu} \tilde{G}^{\mu\nu} \\ & + \frac{if_\psi}{M} \partial_\mu a \bar{\psi} \gamma^\mu \gamma_5 \psi - \dots \end{aligned} \quad (26)$$

Here the term in  $\psi$  denotes possible fermion couplings to the axion  $a$ . The mass scale  $M$  plays the role of the axion decay constant and sets the scale for this new physics. The axion transforms under a new global U(1) symmetry, called Peccei-Quinn symmetry (Peccei and Quinn, 1977),

to cancel the  $\Theta_{\text{QCD}}$  term, with strong CP violation replaced by the axion coupling to gluons and photons. The axion here develops a vacuum expectation value with the potential minimized at  $\langle \text{vac}|a|\text{vac} \rangle / M = \Theta_{\text{QCD}}$ . The mass of the QCD axion is given by (Weinberg, 1996)

$$m_a^2 = \frac{F_\pi^2}{M^2} \frac{m_u m_d}{(m_u + m_d)^2} m_\pi^2. \quad (27)$$

Axions are possible dark matter candidates. Constraints from experiments tells us that  $M$  must be very large. Laboratory based experiments based on the two-photon anomalous couplings of the axion (Ringwald, 2015), ultracold neutron experiments to probe axion to gluon couplings (Abel *et al.*, 2017), together with astrophysics and cosmology constraints suggest a favored QCD axion mass between  $1\mu\text{eV}$  and  $3\text{ meV}$  (Baudis, 2018; Kawasaki and Nakayama, 2013), which is the sensitivity range of the ADMX experiment in Seattle (Rosenberg, 2015), corresponding to  $M$  between about  $6 \times 10^9$  and  $6 \times 10^{12}$  GeV. The small axion interaction strength,  $\sim 1/M$ , means that the small axion mass corresponds to a long lifetime and stable dark matter candidate, *e.g.*, lifetime longer than about the present age of the Universe. If the axions were too heavy they would carry too much energy out of supernova explosions, thereby observably shortening the neutrino arrival pulse length recorded on Earth in contradiction to Sn 1987a data (Kawasaki and Nakayama, 2013). Possible axion candidates would also need to be distinguished from other possible 5th force light mass scalar bosons (Mantry *et al.*, 2014).

### IV. $\eta$ AND $\eta'$ DECAYS

For the  $\eta$  and  $\eta'$  mesons there are two main decay types: hadronic decays to 3 pseudoscalar mesons and electromagnetic decays to two photons. The hadronic decays are sensitive to the details of chiral dynamics and, for decays into 3 pions, the difference in the light up and down quark masses. The two photon decays tell us about the spatial and quark/gluon structure of the mesons with extra (more model dependent) information coming from decays to  $\eta'$  final states (Rosner, 1983). Searches for rare and forbidden decays of the  $\eta$  and  $\eta'$  mesons constrain tests of fundamental symmetries.

The total widths quoted by the Particle Data Group are  $1.31 \pm 0.05$  keV for the  $\eta$  meson and  $0.196 \pm 0.009$  MeV for the  $\eta'$  (Patrignani *et al.*, 2016) with the  $\eta'$  result including the total width value determined directly from the mass distribution measured in proton-proton collisions,  $\Gamma = 0.226 \pm 0.017 \pm 0.014$  MeV (Czerwinski *et al.*, 2010). The main branching ratios for the  $\eta$  decays are  $\eta \rightarrow 3\pi^0$  at  $32.68 \pm 0.23\%$ ,  $\eta \rightarrow \pi^+\pi^-\pi^0$  at  $22.92 \pm 0.28\%$ , and  $39.31 \pm 0.20\%$  for the two photon decay  $\eta \rightarrow 2\gamma$ . For the  $\eta'$  the main decays are  $\eta' \rightarrow \eta\pi^+\pi^-$  at  $42.6 \pm 0.7\%$  and  $\eta' \rightarrow \eta\pi^0\pi^0$  at  $22.8 \pm 0.8\%$  (Patrignani *et al.*, 2016).

## A. Hadronic decays

The  $\eta \rightarrow 3\pi$  decay is of key interest. This process is driven by isospin violation in the QCD Lagrangian, the difference in light-quark up and down quark masses  $m_u \neq m_d$ . In the absence of small (few percent) electromagnetic contributions (Baur *et al.*, 1996), the decay amplitude is proportional to  $m_d - m_u$  which is usually expressed in terms of the ratio

$$\frac{1}{R_m^2} = \frac{m_d^2 - m_u^2}{m_s^2 - \hat{m}^2} \quad (28)$$

where  $\hat{m} = \frac{1}{2}(m_d + m_u)$  and  $m_s$  is the strange quark mass. Expansion in chiral perturbation theory (in the light-quark masses) converges slowly due to final state pion rescattering effects. Fortunately, these can be resummed using dispersive techniques allowing one to make a precise determination of the ratio of light quark masses from experiments, for a review see Leutwyler (2013).

Recent accurate measurements of the  $\eta$  decay to charged pions,  $\eta \rightarrow \pi^+\pi^-\pi^0$ , have been performed by the WASA-at-COSY experiment at FZ-Jülich (Adlarson *et al.*, 2014b), the KLOE-2 Collaboration at LN-Frascati (Anastasi *et al.*, 2016) and at BES in Beijing (Ablikim *et al.*, 2017). The neutral 3 pion decay  $\eta \rightarrow 3\pi^0$  has most recently been measured by WASA (Adolph *et al.*, 2009), KLOE (Ambrosino *et al.*, 2011), the Mainz A2 Collaboration (Prakhov *et al.*, 2018) and at BES (Ablikim *et al.*, 2015a).

Taking the precise data on  $\eta \rightarrow \pi^+\pi^-\pi^0$  from KLOE-2 as input, Colangelo *et al.* (2017) find  $R_m = 22.0 \pm 0.7$ . Combining this result with  $m_s/\hat{m} = 27.30(34)$  quoted in the lattice Ref. (Aoki *et al.*, 2017), they obtain the light quark mass ratio  $m_u/m_d = 0.44(3)$ . Similar results have been obtained by Guo *et al.* (2017) who include both KLOE-2 and WASA data for this decay and get  $R_m = 21.6 \pm 1.1$ . Similar values for  $R_m$  were found using earlier data by Kambor *et al.* (1996) and Kampf *et al.* (2011). These numbers compare with  $R_m = 23.9$  which follows from the simple leading-order calculation in Eq. (8).

The decay  $\eta' \rightarrow 3\pi$  is also driven by isospin violation. In addition to the QCD processes involved in the  $\eta$  decay, here there are also important contributions from the sub-processes  $\eta' \rightarrow \eta\pi\pi$  plus  $\eta\pi^0$  mixing to give the 3 pion final state and  $\eta' \rightarrow \pi\rho$  with  $\rho \rightarrow \pi\pi$ .

These decays contrast with the process  $\eta' \rightarrow \eta\pi\pi$  which is the dominant  $\eta'$  decay with leading QCD term not driven by the difference in  $m_u$  and  $m_d$ . Here the singlet component in both the initial and final state isoscalar mesons  $\eta'$  and  $\eta$  through  $\eta - \eta'$  mixing means that the reaction is potentially sensitive also to OZI-violating couplings, *e.g.*, from the  $Q^2\partial^\mu\pi_a\partial_\mu\pi_a$  term at next-to-leading order in  $1/N_c$  in the chiral Lagrangian. The leading order amplitude for this decay is proportional to  $m_\pi^2$  and vanishes in the chiral limit. The large

branching ratios for this decay tell us that non-leading terms play a vital role.

We refer to the lectures of Kupsc (2009) for further details of the analysis of these processes and to Fang *et al.* (2018) for a review of the latest experimental results from the BES experiment, as well as earlier measurements of these decays.

## B. Two-photon interactions

The two photon decays of the  $\pi^0$ ,  $\eta$  and  $\eta'$  mesons are driven by the QED axial anomaly.

For the  $\pi^0$ , in the chiral limit

$$F_\pi g_{\pi^0\gamma\gamma} = \frac{N_c}{3\pi}\alpha \quad (29)$$

where  $g_{\pi^0\gamma\gamma}$  is the  $\pi^0$  two-photon coupling,  $N_c$  is the number of colors (=3) and  $\alpha$  is the electromagnetic coupling. Without the QED anomaly the decay amplitude would be proportional to  $m_\pi^2$  and vanish for massless quarks.

For the isoscalar mesons one also has to consider the QCD gluon axial anomaly. In the chiral limit one finds the relation (Shore and Veneziano, 1992)

$$F_0 \left[ g_{\eta'\gamma\gamma} + \frac{1}{N_f} F_0 m_\eta^2 g_{Q\gamma\gamma}(0) \right] = \frac{4N_c}{3\pi}\alpha. \quad (30)$$

Here  $g_{\eta'\gamma\gamma}$  and  $g_{Q\gamma\gamma}$  denote the two photon couplings of the physical  $\eta'$  and topological charge density term. Chiral corrections are discussed in Shore (2006) within the context of the two mixing angle scheme. The observed decay rates for the  $\eta$  and  $\eta'$  suggest small gluonic coupling,  $g_{Q\gamma\gamma} \sim 0$ , with the gluonic term contributing at most 10% of the  $\eta'$  decay (Shore, 2006). Most accurate measurements of the  $\eta \rightarrow \gamma\gamma$  and  $\eta' \rightarrow \gamma\gamma$  decays come from KLOE-2 (Babusci *et al.*, 2013a) and BELLE (Adachi *et al.*, 2008) respectively.

When one or both of the photons becomes virtual, the pseudoscalar meson coupling to two photon amplitudes involve transition form factors  $F_{P\gamma}(q^2)$  associated with the spatial structure of the mesons.

There are measurements in both space-like,  $Q^2 = -q^2 > 0$ , and time-like,  $q^2 > 0$ , kinematics where  $q$  is the four-momentum transfer in the reaction<sup>4</sup>. The space-like region can be studied through  $\gamma\gamma^* \rightarrow P$  fusion processes in electron-positron collisions, with  $\eta$  and  $\eta'$  production data from CELLO (Behrend *et al.*, 1991), CLEO (Gronberg *et al.*, 1998), BABAR (del Amo Sanchez *et al.*,

<sup>4</sup> Here  $Q^2$  denotes the squared four-momentum transfer of the virtual photon and should not be confused with “ $Q$ ” in our previous discussion where it denoted the topological charge density. For consistency with the literature we here keep  $Q$  for both cases.

2011) and KLOE-2 (Babusci *et al.*, 2013a). The time-like region is studied in meson decays  $P \rightarrow \gamma\gamma^*$ ,  $\gamma^* \rightarrow l^+l^-$ , *e.g.*, Dalitz decays to lepton pairs in the final state with positive  $q^2$  equal to the invariant mass of the final state lepton pair  $l^+l^-$ . Single and double Dalitz decays can be studied. Recent measurements for the  $\eta$  come from the A2 Collaboration at Mainz (Adlarson *et al.*, 2017a), WASA-at-COSY (Adlarson *et al.*, 2016), and NA60 at CERN (Arnaldi *et al.*, 2009), with data from BES-III (Ablikim *et al.*, 2015b) for the  $\eta'$ .

Production of a pseudoscalar meson  $P$  through fusion of a real and deeply virtual photon,  $\gamma\gamma^* \rightarrow P$ , are described by perturbative QCD in terms of light-front wavefunctions (Feldmann and Kroll, 1998; Lepage and Brodsky, 1980). In the asymptotic large  $Q^2$  limit, the transition form-factors for  $\gamma\gamma^* \rightarrow P$

$$Q^2 F_{P\gamma}(Q^2) \rightarrow 6 \sum_a C_a f_P^a \quad (Q^2 \rightarrow \infty). \quad (31)$$

Here, mixing is encoded in the decay constants  $f_P^a$  and  $C_a$  are the quark charge factors. The light-cone wavefunctions  $\Psi_P^a(x, \vec{k}_t)$  describe the amplitude for finding a quark-antiquark pair carrying light-cone momentum fraction  $x$  and  $(1-x)$  and transverse momentum  $\vec{k}_t$ . These amplitudes are normalized via

$$\int \frac{d^2\vec{k}_t}{16\pi^3} \int_0^1 dx \Psi_P^a(x, \vec{k}_t) = \frac{f_P^a}{2\sqrt{6}}. \quad (32)$$

As we explained in Section II, one cannot separate an anomalous  $K_\mu$  contribution from  $F_0$  when working with gauge invariant observables, *e.g.*, using  $\overline{\text{MS}}$  renormalization. The small OZI-violation in  $F_0$  is consistent with RG effects and with the quark-antiquark leading Fock component moving in a topological gluon potential. Glue may be (strongly) excited in the intermediate states of hadronic reactions.

The low  $q^2$  region is described using form-factors

$$F(q^2) = F(0) \frac{\Lambda^2}{\Lambda^2 - q^2 - i\Gamma\Lambda}. \quad (33)$$

The slope parameter

$$b_P = \left. \frac{d|F(q^2)|}{dq^2} \right|_{q^2=0} = F(0) \frac{1}{\Lambda^2 + \Gamma^2} \quad (34)$$

is often quoted for the decays. Values extracted for the  $\eta'$  from timelike decays are  $b_{\eta'} = 1.60 \pm 0.17 \pm 0.08 \text{ GeV}^{-2}$  and  $\Lambda = 0.79 \pm 0.04 \pm 0.02 \text{ GeV}$  from BES-III (Ablikim *et al.*, 2015b), with  $\Lambda$  close to the  $\omega$  and  $\rho$  masses which appear with vector meson dominance of the virtual photon. In the space-like region the CELLO Collaboration found  $b_{\eta'} = 1.60 \pm 0.16 \text{ GeV}^{-2}$  (Behrend *et al.*, 1991). Note that the  $\Gamma$  width term is important here for the  $\eta'$  because of its large mass and short life time. For the  $\eta$  slope measured in time-like decays, the most precise

measurement of  $\Lambda_\eta^{-2}$  is  $1.97 \pm 0.11 \text{ GeV}^{-2}$  from the A2 Collaboration at Mainz (Adlarson *et al.*, 2017a).

Extending the final states from charged leptons to charged pions, the process  $\eta \rightarrow \pi^+\pi^-\gamma$  includes contributions from both the transition form-factor and also the box anomaly shown in Fig. 3. Recent measurements are from WASA (Adlarson *et al.*, 2012) and KLOE-2 (Babusci *et al.*, 2013b). For a recent theoretical discussion see Kubis and Plenler (2015).

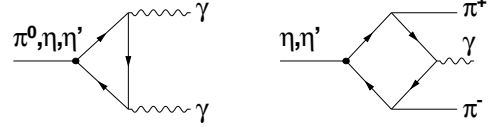


FIG. 3 Feynman diagrams for the triangle and box anomalies. The anomaly comes from the point-like part of the quark loop with the quarks carrying maximum momentum in the loop.

The  $\eta'\gamma$  transition form factor for deeply virtual  $\gamma^*\gamma \rightarrow \eta'$  was interpreted in (Kroll and Passek-Kumericki, 2013) to give a quite large (radiatively generated) two gluon Fock component in the  $\eta'$  wavefunction. In this calculation the glue enters at next-to-leading order. Exclusive central production of the  $\eta'$  in high-energy proton-proton collisions at the LHC has been suggested as a cleaner probe since here the glue enters at leading-order (Harland-Lang *et al.*, 2013).

In lower energy experiments, quark model inspired fits including a “gluonium admixture” (Rosner, 1983) have been performed to various low energy processes including the  $\phi \rightarrow \eta'\gamma$  decay by the KLOE Collaboration (Ambrosino *et al.*, 2007, 2009; Gauzzi, 2012) suggesting a phenomenological “gluonium fraction” of  $0.12 \pm 0.04$ . Various theoretical groups’ analyses of the same data suggest values between zero and about 10% depending on form-factors that are used in the fits (Di Donato *et al.*, 2012; Escribano and Nadal, 2007; Thomas, 2007). When trying to extract a “gluonic content” from experiments it is important to be careful what assumptions about glue have gone into the analyses. Photon coupling decay processes are theoretically cleaner with less model dependence in their interpretation.

At high energies, heavy-quark meson decays to light-quark states including the  $\eta'$  proceed through OZI-violating gluonic intermediate states, *e.g.*,  $J/\Psi$  to  $\eta'\gamma$  and  $\eta\gamma$  giving experimental constraints on the flavor-singlet components in these mesons. In high energy processes large branching ratios for  $D_s$  and  $B$  meson decays to  $\eta'$  final states have been observed and are believed to be driven in part by coupling to gluonic intermediate states (Atwood and Soni, 1997; Aubert *et al.*, 2001; Bali *et al.*, 2015; Ball *et al.*, 1996; Behrens *et al.*, 1998; Browder *et al.*, 1998; Dighe *et al.*, 1996, 1997; Fritzsche, 1997; Hou and Tseng, 1998).

### C. Precision tests of fundamental symmetries

Precision measurements of the muon's anomalous magnetic moment  $a_\mu = (g-2)/2$  are an important test of the Standard Model. The anomalous magnetic moment is induced by quantum radiative corrections to the magnetic moment with  $g$  the proportionality constant between the particle's magnetic moment and its spin. The present experimental value from BNL (Bennett *et al.*, 2006)

$$a_\mu^{\text{exp}} = (11659209.1 \pm 5.4 \pm 3.3) \times 10^{-10} \quad (35)$$

differs from the present best theoretical expectation by

$$a_\mu^{\text{exp}} - a_\mu^{\text{th}} = (31.3 \pm 7.7) \times 10^{-10} \quad (36)$$

– a 4.1  $\sigma$  deviation (Jegerlehner, 2017). This result is a puzzle also since possible new physics contributions which might have resolved the discrepancy are now seriously challenged by LHC data which are, so far, consistent with the Standard Model and no extra new particles in the mass range of the experiments. New experiments at Fermilab and J-PARC plan to check this result with the Fermilab experiment improving the present statistical error on  $a_\mu$  from 540 to 140 ppb or  $1.4 \times 10^{-10}$  (Hertzog, 2016).

One key issue is the size of low-energy QCD hadronic contributions to the muon  $g-2$ . These are the biggest source of theoretical uncertainty in the Standard Model prediction with one important ingredient being the hadronic contributions to virtual photon-photon scattering with meson intermediate states. These are sensitive to the  $\pi^0$ ,  $\eta$  and  $\eta'$  transition form-factors. Various calculations appear in the literature; see Table 5.13, page 474, in Jegerlehner (2017). Contributions to  $a_\mu$  from the  $\eta$  and  $\eta'$  are typically about  $3 \times 10^{-10}$  with pion contributions between about 5 and  $8 \times 10^{-10}$ . The total hadronic contribution to  $a_\mu$  including vacuum polarization effects is about  $690 \times 10^{-10}$  with a net light-by-light contribution of about  $10 \times 10^{-10}$  after summing over terms with positive and negative signs.

Studies of  $\eta$  meson decays also provide new precision tests of discrete symmetries: charge conjugation,  $C$ , and charge-parity,  $CP$  (Jarlskog and Shabalin, 2002). The  $\eta$  and  $\eta'$  mesons are eigenstates of parity  $P$ , charge conjugation and combined  $CP$  parity with eigenvalues  $P = -1$ ,  $C = +1$  and  $CP = -1$ .  $C$  tests include searches for forbidden decays to an odd number of photons. *e.g.*,  $\eta \rightarrow 3\gamma$  (Nefkens *et al.*, 2005a),  $\eta \rightarrow \pi^0\gamma$  (which is also forbidden by angular momentum conservation) (Adlarson *et al.*, 2018a), and  $\eta \rightarrow 2\pi^0\gamma$  (Nefkens *et al.*, 2005b). Charge conjugation invariance has also been tested in the  $\eta \rightarrow \pi^0\pi^+\pi^-$  decay. Here  $C$  violation can manifest itself as an asymmetry in the energy distributions for  $\pi^+$  and  $\pi^-$  mesons in the rest frame of the  $\eta$  meson. The results were found consistent with zero (Adlarson *et al.*, 2014b). A possible  $CP$  violating asymmetry

in the  $\eta \rightarrow \pi^+\pi^-e^+e^-$  decay was determined consistent with zero (Adlarson *et al.*, 2016).

### V. $\eta$ - AND $\eta'$ -NUCLEON INTERACTIONS

Close-to-threshold  $\eta$  and  $\eta'$  production is studied in photon-nucleon and proton-nucleon collisions. Photon induced reactions are important for studies of nucleon resonance excitations; for a recent review see Krusche and Wilkin (2014).  $\eta$  meson production is characterized by the strong role of the s-wave  $N^*(1535)$  resonance. For studies of higher mass excited resonances, recent advances with double polarization observables are playing a vital role. Recent measurements for the  $\eta$  come from Mainz (Witthauer *et al.*, 2016, 2017), Jefferson Laboratory (Al Ghouli *et al.*, 2017; Senderovich *et al.*, 2016) and GrAAL (Levi Sandri *et al.*, 2015), with partial wave analysis studies reported in Anisovich *et al.* (2015).

For the  $\eta'$ , (quasi-free) photoproduction from proton and deuteron targets has been studied at ELSA (Crede *et al.*, 2009; Jaegle *et al.*, 2011; Krusche, 2012), MAMI (Kashevarov *et al.*, 2017) and by the CLAS experiment at Jefferson Laboratory (Dugger *et al.*, 2006; Williams *et al.*, 2009) with new double polarization observables reported in Collins *et al.* (2017). The production cross-section is isospin independent for incident photon energies greater than 2 GeV, where  $t$ -channel exchanges are important. At lower energies, particularly between 1.6 and 1.9 GeV where the proton cross-section peaks, the proton and quasi-free neutron cross-sections show different behavior. These data have recently been used in partial wave analysis revealing strong indications of four excited nucleon resonances contributing to the  $\eta'$  production process:  $N(1895)\frac{1}{2}^-$ ,  $N(1900)\frac{3}{2}^+$ ,  $N(2100)\frac{1}{2}^+$ , and  $N(2120)\frac{3}{2}^-$ . Details including the branching ratios for coupling to the  $\eta'$  are given in Anisovich *et al.* (2017).

In proton-nucleon collisions the  $\eta$  and  $\eta'$  production processes proceed through exchange of a complete set of virtual meson hadronic states, which in models is usually truncated to single virtual meson-exchange, *e.g.*,  $\pi$ ,  $\eta$ ,  $\rho$ ,  $\omega$  and  $\sigma$  (correlated two-pion) exchanges (Deloff, 2004; Faldt and Wilkin, 2001; Nakayama *et al.*, 2003; Pena *et al.*, 2001; Shyam, 2007). For the  $\eta'$  OZI-violating production is also possible through excitation of non-perturbative glue in the interaction region (Bass, 1999). The exchange process can also induce nucleon resonance excitation, especially the  $N^*(1535)$  with  $\eta$  production, before final emission of the  $\eta$  or  $\eta'$  meson. The production mechanism is studied through measurements of the total and differential cross-sections, varying the isospin of the second nucleon and polarization observables with one of the incident protons transversely polarized (Moskal, 2004). The interpretation of these processes is sensitive to the choice of exchanged mesons and nucleon resonances included in the models and the truncation of the

virtual exchange contributions which affects, *e.g.*, the meson nucleon form-factors in the calculations.

The near-threshold  $\eta$  meson production in nucleon-nucleon collisions has been investigated extensively in the CELSIUS, COSY and SATURNE facilities. The results determined by different experiments for the total (Bergdolt *et al.*, 1993; Calen *et al.*, 1996; Chiavassa *et al.*, 1994; Hibou *et al.*, 1998; Moskal *et al.*, 2004, 2010; Smyrski *et al.*, 2000) and differential (Abdel-Bary *et al.*, 2003; Moskal *et al.*, 2004, 2010; Petren *et al.*, 2010) cross-sections for the  $pp \rightarrow pp\eta$  and for the quasi-free  $pn \rightarrow pn\eta$  reactions (Calen *et al.*, 1996, 1998; Moskal *et al.*, 2009) are consistent within the estimated uncertainties. In the different experiments  $\eta$  mesons could be produced up to excess energy  $\mathcal{E}$  of 92 MeV at CELSIUS, 502 MeV at COSY and 593 MeV at SATURNE.

$\eta'$  production has been measured in proton-proton collisions close-to-threshold (excess energy  $\mathcal{E}$  between 0.76 and  $\sim 50$  MeV) by the COSY-11 collaboration at FZ-Jülich (Czerwinski *et al.*, 2014a; Khoukaz *et al.*, 2004; Klaja *et al.*, 2010b; Moskal *et al.*, 1998, 2000a,b) and at  $\mathcal{E} = 3.7$  MeV and 8.3 MeV by SPESIII (Hibou *et al.*, 1998) and 144 MeV by the DISTO Collaboration at SATURNE (Balestra *et al.*, 2000).

For near-threshold meson production, the cross-section is reduced by initial state interaction between the incident nucleons and enhanced by final state interactions between the outgoing hadrons. For comparing production dynamics a natural variable is the volume of available phase space which is approximately independent of the meson mass. Making this comparison for the neutral pseudoscalar mesons, it was found that production of the  $\eta$  meson is about six times enhanced compared to the  $\pi^0$  which is six times further enhanced compared to the  $\eta'$ . The production amplitudes for the  $\pi^0$  and  $\eta'$  have the same (nearly constant) dependence on the phase space volume in the measured kinematics close-to-threshold, whereas the production amplitude for the  $\eta$  exhibits possible growth with decreasing phase space volume due to strong  $\eta$ -proton attractive interaction (Moskal *et al.*, 2000b). The large  $\eta$  production cross-section is driven by strong coupling to the  $N^*(1535)$ . In Fig. 4 we show the  $\eta$  and  $\eta'$  production total cross-section data as a function of excess energy. The Figure also shows the curves expected if one includes only the  $s$ -wave and final state interaction in the proton-proton in the simplest approximation (Faeldt and Wilkin, 1996; Wilkin, 2016):

$$\sigma_T(pp \rightarrow pp\eta) = C \left( \frac{\mathcal{E}}{\mu} \right)^2 \left/ \left( 1 + \sqrt{1 + \mathcal{E}/\mu} \right)^2 \right. . \quad (37)$$

Here the excess energy  $\mathcal{E} = W - (2m_p + m)$ , with  $W$  the total center of mass energy,  $m_p$  the proton mass and  $m$  the meson mass. The constant  $C$  depends upon the reaction mechanism and can be adjusted to fit the data. Strong  $\eta$ -nucleon final state interaction is seen at the

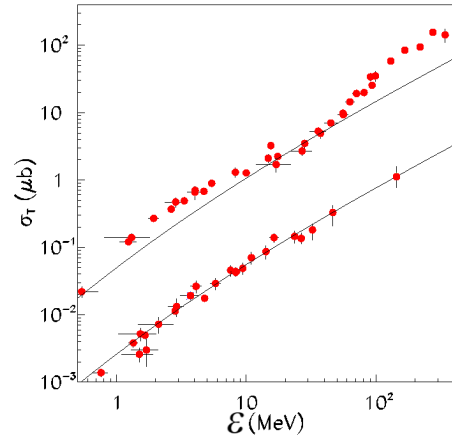


FIG. 4 World data for the total cross sections for  $pp \rightarrow pp\eta$  (upper points) and  $pp \rightarrow pp\eta'$  (lower points) – see text. The solid curves are arbitrarily scaled  $pp$  FSI predictions of Eq. (37). The Figure is adapted from Wilkin (2016).

lowest  $\mathcal{E}$  with deviation of the data from the theoretical curve, much stronger than for the  $\eta'$ . Deviations at large  $\mathcal{E}$  are likely to originate from higher partial waves in the final proton-proton system. The pole parameter  $\mu$  fitted from experiment is  $\approx 0.75$  MeV for the  $\eta'$  (Wilkin, 2016).

Measurements of the differential cross-sections for  $\eta$  production at  $\mathcal{E} = 15.5$  MeV (Moskal *et al.*, 2004) and at  $\mathcal{E} = 41$  MeV (Abdel-Bary *et al.*, 2003) are consistent with isotropic  $\eta$  production within the statistical errors, though at 41 MeV the accuracy of the data do not exclude a few per cent contribution from higher partial waves. For  $\eta'$  production, the differential cross sections measured at SATURNE (Balestra *et al.*, 2000) at  $\mathcal{E} = 143.8$  MeV and at COSY (Khoukaz *et al.*, 2004) at  $\mathcal{E} = 46.6$  MeV are consistent with pure  $Ss$ -wave production with  $\approx 10\%$  level higher partial wave contributions possible within the experimental uncertainties. Here  $Ss$  denotes the outgoing protons in  $S$ -wave in their rest frame and the meson is in  $s$ -wave relative to the center-of-mass.

Values for the real part of the  $\eta$ -nucleon scattering length  $a_{\eta N}$  have been obtained between 0.2 fm and 1.05 fm depending on the analysis, including whether the  $\eta$ - $\eta'$  mixing angle is constrained or not. Fits to experimental data suggest a value close to 0.9 fm for the real part of  $a_{\eta N}$  (Arndt *et al.*, 2005; Green and Wycech, 1999, 2005). In contrast, smaller values of  $a_{\eta N}$  with real part  $\sim 0.2$  fm are predicted by chiral coupled-channel models where the  $\eta$  meson is treated in pure octet approximation (Garcia-Recio *et al.*, 2002; Inoue and Oset, 2002; Waas and Weise, 1997).

The scattering length  $a_{\eta N}$  is much greater than the scattering length for pion-nucleon scattering. Pion nucleon interactions are dominated by the  $p$ -wave  $\Delta$  (lightest mass) nucleon resonance excitation with small scattering length, which for the  $\pi^0$  the real part is  $a_{\pi N} =$

$0.1294 \pm 0.0009$  fm (Sigg *et al.*, 1996).

The COSY-11 collaboration have recently made a first measurement of the  $\eta'$ -nucleon scattering length in free space,

$$a_{\eta'p} = (0 \pm 0.43) + i(0.37 \pm_{-0.16}^{+0.40}) \text{ fm} \quad (38)$$

from studies of the  $\eta'$  final state interaction in  $\eta'$  production in proton-proton collisions close-to-threshold (Czerwinski *et al.*, 2014b). This value was extracted from fitting the low  $\mathcal{E}$  data,  $\mathcal{E}$  up to 11 MeV, where the cross-section is clearly  $s$ -wave dominated. A recent extraction from photoproduction data gives

$$|a_{\eta'N}| = 0.403 \pm 0.015 \pm 0.060 \text{ fm} \quad (39)$$

with phase  $87 \pm 2^\circ$  (Anisovich *et al.*, 2018). Theoretical models in general prefer a positive sign for the real part of  $a_{\eta'p}$  corresponding to attractive interaction. The meson-nucleon scattering lengths are also related to the corresponding meson-nucleus optical potential; see Section VI below. Measurements of the  $\eta'$  mass shift in carbon favor a value for the real part of  $a_{\eta'N}$  of about 0.5 fm.

These numbers can be understood in terms of the underlying dynamics. In chiral dynamics, the Goldstone-boson nucleon scattering lengths are proportional at tree level to the meson mass squared, *e.g.*, the Tomozawa-Weinberg relation (Ericson and Weise, 1988). For pion-nucleon scattering, the nearest  $s$ -wave resonance is the  $N^*(1535)$ , which is too far away to affect the near-threshold interaction. For the  $\eta$  one finds a strong effect from the close-to-threshold resonance  $N^*(1535)$ . With the  $\eta'$ , the meson mass squared is large through the gluonic mass term  $\tilde{m}_{\eta_0}^2$ . The tree level scattering length is non-vanishing in the chiral limit.

Measurements of the isospin dependence of  $\eta$  meson production in proton-nucleon collisions revealed that the total cross-section for the quasi-free  $pn \rightarrow pn\eta$  reaction exceeds the corresponding cross section for  $pp \rightarrow pp\eta$  by a factor of about three at threshold and by factor of six at higher excess energies between about 25 and 100 MeV (Calen *et al.*, 1998; Moskal *et al.*, 2009). The strong isospin dependence tells us there must be a significant isovector exchange contribution at work in the proton-nucleon collisions.

The spin analyzing power  $A_y$  for  $\eta$  meson production in proton-proton collisions close-to-threshold with one proton beam transversely polarized has recently been measured with high statistics by the WASA-at-COSY Collaboration (Adlarson *et al.*, 2018b). The analyzing power is found to be consistent with zero for an excess energy of  $\mathcal{E} = 15$  MeV signaling  $s$  wave production with no evidence for higher partial waves. This result is in contrast with meson-exchange model predictions which had anticipated asymmetries up to about 20 % based on  $\pi$  or  $\rho$  exchange dominance in the interaction (Faldt and Wilkin,

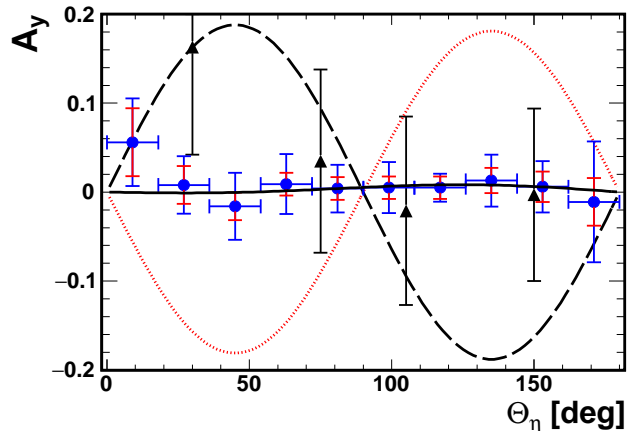


FIG. 5 Analyzing power for the  $\bar{p}p \rightarrow pp\eta$  reaction at  $Q = 15$  MeV. Here  $\theta_\eta$  is the polar angle for the emission of the  $\eta$  meson in the center of mass system. Full circles represent WASA results (Adlarson *et al.*, 2018b). Triangles are early data from COSY-11 measured at  $\mathcal{E} = 10$  MeV (Czyzykiewicz *et al.*, 2007). The dotted line denotes the prediction based on pseudoscalar-meson-exchange (Nakayama *et al.*, 2003), whereas the dashed line represents the vector exchange model (Faldt and Wilkin, 2001). The solid line is the partial-waves fit to the WASA data. The Figure is adapted from Adlarson *et al.* (2018b).

2001; Nakayama *et al.*, 2003); see Fig. 5. At  $\mathcal{E} = 72$  MeV the data reveal strong interference of  $Ps$  and  $Pp$  partial waves and cancellation of  $(Pp)^2$  and  $Ss * Sd$  contributions (Adlarson *et al.*, 2018b). Different meson-exchanges induce very different spin dependence in the production process. Polarized beams and measurement of the analyzing power can therefore put powerful new constraints on theoretical understanding of the  $\eta$  production process. A possible explanation of the vanishing analyzing power at 15 MeV might be cancellation with destructive interference between  $\pi$  and  $\rho$  exchanges in  $\eta$  production very close-to-threshold together with a strong (spin independent) scalar  $\sigma$  (correlated two pion) exchange contribution. In this scenario one would expect to see a finite analyzing power in proton-neutron collisions given the strong isospin dependence to the production mechanism.

Measurements of the isospin dependence of  $\eta'$  production suggest a different production mechanism for this meson (Klaaja *et al.*, 2010a; Moskal *et al.*, 2000b). Using the quasi-free proton-neutron interaction (Moskal *et al.*, 2006) COSY-11 placed an upper bound on  $\sigma(pn \rightarrow pn\eta')$  and the ratio  $R_{\eta'} = \sigma(pn \rightarrow pn\eta')/\sigma(pp \rightarrow pp\eta')$  (Klaaja *et al.*, 2010a). For excess energy between 8-24 MeV the upper limit of  $R_{\eta'}$  was observed to be consistently one standard deviation below the corresponding ratio for  $\eta$  production (Moskal *et al.*, 2009). In the theoretical limit that  $\eta'$  production proceeds entirely through gluonic excitation in the intermediate state this ratio would go to one. The data are consistent with both a role for OZI-violating  $\eta'$  production (Bass, 1999, 2000) and the meson-

exchange model (Kaptari and Kampfer, 2008).

The observed  $s$ -wave dominance of  $\eta$  and  $\eta'$  production in a large kinematic range close-to-threshold might also, in part, be understood in terms of the phenomenology of Gell-Mann and Watson (1954). If the strength of the primary production partial amplitudes were constant over the phase space, then the energy dependence of the partial cross sections would be given by

$$\sigma_{Ll} \propto q_{max}^{2L+2l+4} \propto \eta_M^{2L+2l+4}. \quad (40)$$

Here  $\eta_M = q_{max}/m$  with  $m$  and  $q_{max}$  the mass and maximum momentum of the created meson. Close-to-threshold the  $Ss$  partial-wave cross-section should increase with the fourth power of  $\eta_M$  which, non-relativistically, is related to the excess energy by  $\mathcal{E} = \eta_M^2 m(2m_p + m)/4m_p$ . The orbital angular momentum  $l$  of the produced meson is  $l = Rq \sim q/m$ , where  $R$  is a characteristic distance from the center of the collision  $R \sim 1/m \sim 1/\Delta p$  with  $m$  the meson mass and  $\Delta p$  the momentum transfer between the colliding nucleons. Hence  $\eta_M$  denotes the classically calculated maximum angular momentum of the meson in the center of mass frame.

Investigations with polarized beams and targets (Meyer *et al.*, 1999, 2001) of the  $\bar{p}\bar{p} \rightarrow pp\pi^0$  reaction tell us that the  $Ss$  partial-wave accounts for more than 95% of the total cross section up to  $\eta_M \approx 0.4$ . Extending this phenomenology to heavy mesons suggests that the  $Ss$  partial wave combination will constitute the overwhelming fraction of the total production cross-section for  $\eta_M$  smaller than about 0.4 for constant production amplitudes  $|M_{Ll}^0|$ . That is, one expects the heavier  $\eta$  and  $\eta'$  mesons to be produced predominantly via the  $Ss$  state in a much larger excess energy range and hence larger phase space volume. Whereas for  $\pi^0$  production the onset of higher partial waves is observed at  $\mathcal{E}$  around 10 MeV, it is expected only above 100 MeV for the  $\eta'$  and above  $\approx 40$  MeV for the  $\eta$  meson (modulo the possible small change in amplitude with increasing phase space volume (Klaja *et al.*, 2010b; Moskal *et al.*, 2000b)).

### A. The N\*(1535) resonance and its structure

The internal structure of the N\*(1535) has been a hot topic of discussion. In quark models the N\*(1535) is interpreted as a 3-quark state:  $(1s)^2(1p)$ . One finds configuration mixing with the N\*(1650) between  $|^2P_{\frac{1}{2}}\rangle$  and  $|^4P_{\frac{1}{2}}\rangle$  states (with spin  $\frac{1}{2}$  and  $\frac{3}{2}$  respectively, orbital angular momentum  $L = 1$  and total angular momentum  $J = \frac{1}{2}$ ) (Isgur and Karl, 1978). Recent QCD lattice calculations support a 3-quark state, with couplings to 5 quark components and probability of about 50% to contain the bare baryon (Liu *et al.*, 2016). This contrasts with the  $\Lambda(1405)$  resonance which is understood as dynamically

generated in the kaon-nucleon system (Hall *et al.*, 2015). The structure of the N\*(1535) has also been discussed within chiral coupled-channel models (Garzon and Oset, 2015; Hyodo *et al.*, 2008; Inoue *et al.*, 2002; Kaiser *et al.*, 1995). Here the N\*(1535) and N\*(1650) are explained as a  $K\Sigma$  state together with strong vector meson component (Garzon and Oset, 2015). These coupled-channel model calculations are performed with the  $\eta$  treated as a pure octet state. In Jefferson Laboratory measurements, the N\*(1535) contribution to  $\eta$  electroproduction was observed to fall away more slowly with increasing large  $Q^2$  (up to about 7 GeV<sup>2</sup>) than expected for a meson-baryon bound system (Armstrong *et al.*, 1999; Aznauryan and Burkert, 2012; Burkert, 2018; Dalton *et al.*, 2009). This suggests a significant 3-quark contribution. On the other hand, the low  $Q^2$  (below 1 GeV<sup>2</sup>) longitudinal transition amplitude suggests the need for meson cloud or other  $4q\bar{q}$  contributions to the N\*(1535) wavefunction.

The branching ratios for the N\*(1535) to decay to  $\eta$ -nucleon and pion-nucleon final states are approximately equal, about 45%. This result is interpreted in Olbrich *et al.* (2018) as evidence for a possible gluon anomaly contribution to the decay. The strong  $\eta$  coupling has also been interpreted in quark models with configuration mixing between the N\*(1535) and N\*(1650) (Chiang *et al.*, 2003; Saghai and Li, 2001).

## VI. THE $\eta$ AND $\eta'$ IN NUCLEI

There is presently vigorous experimental and theoretical activity aimed at understanding the  $\eta$  and  $\eta'$  in medium and to search for evidence of possible  $\eta$  and  $\eta'$  bound states in nuclei. Medium modifications need to be understood self-consistently within the interplay of confinement, spontaneous chiral symmetry breaking and axial U(1) dynamics. In the limit of chiral restoration the pion decay constant  $f_\pi$  should go to zero and (perhaps) with scalar confinement the pion constituent-quark and pion nucleon coupling constants should vanish with dissolution of the pion wavefunction.

One finds a small pion mass shift of order a few MeV in nuclear matter (Kienle and Yamazaki, 2004). Experiments with deeply bound pionic atoms reveal a reduction in the value of the pion decay constant  $f_\pi^{*2}/f_\pi^2 = 0.64 \pm 0.06$  at nuclear matter density (Suzuki *et al.*, 2004). Kaons are observed to experience an effective mass drop for the  $K^-$  to about 270 MeV at two times nuclear matter density in heavy-ion collisions (Barth *et al.*, 1997; Schroter *et al.*, 1994). These heavy-ion experiments also suggest the effective mass of antiprotons is reduced by about 100-150 MeV below their mass in free space (Schroter *et al.*, 1994). What should we expect for the  $\eta$  and  $\eta'$ ? How does the gluonic part of their mass change in nuclei?

Meson masses in nuclei are determined from the me-



son nucleus optical potential and the scalar induced contribution to the meson propagator evaluated at zero three-momentum,  $\vec{k} = 0$ , in the nuclear medium. Let  $k = (E, \vec{k})$  and  $m$  denote the four-momentum and mass of the meson in free space. Then, one solves the equation

$$k^2 - m^2 = \text{Re } \Pi(E, \vec{k}, \rho) \quad (41)$$

for  $\vec{k} = 0$  where  $\Pi$  is the in-medium  $s$ -wave meson self-energy and  $\rho$  is the nuclear density. Contributions to the in medium mass come from coupling to the scalar  $\sigma$  field in the nucleus in mean field approximation, nucleon-hole and resonance-hole excitations in the medium. For  $\vec{k} = 0$ ,  $k^2 - m^2 \sim 2m(m^* - m)$  where  $m^*$  is the effective mass in the medium. The mass shift  $m^* - m$  is the depth or real part of the meson nucleus optical potential. The imaginary part of the potential measures the width of the meson in the nuclear medium. The  $s$ -wave self-energy can be written as (Ericson and Weise, 1988)

$$\Pi(E, \vec{k}, \rho) \Big|_{\{\vec{k}=0\}} = -4\pi\rho \left( \frac{b}{1 + b\langle\frac{1}{r}\rangle} \right). \quad (42)$$

Here  $b = a(1 + \frac{m}{M})$  where  $a$  is the meson-nucleon scattering length,  $M$  is the nucleon mass and  $\langle\frac{1}{r}\rangle$  is the inverse correlation length,  $\langle\frac{1}{r}\rangle \simeq m_\pi$  for nuclear matter density. Attraction corresponds to positive values of  $a$ . The denominator in Eq. (42) is the Ericson-Ericson-Lorentz-Lorenz double scattering correction.

Studies involving bound state searches and excitation functions of mesons in photoproduction from nuclear targets give information about the meson nucleus optical potential.

With a strong attractive interaction there is a chance to form meson bound states in nuclei (Haider and Liu, 1986). If found, these mesic nuclei would be a new state of matter bound just by the strong interaction. They differ from mesonic atoms (Yamazaki *et al.*, 1996) where, for example, a  $\pi^-$  is trapped in the Coulomb potential of the nucleus and bound by the electromagnetic interaction (Toki *et al.*, 1989).

Early experiments with low statistics using photon (Baskov *et al.*, 2012; Pheron *et al.*, 2012), pion (Chrien *et al.*, 1988), proton (Budzanowski *et al.*, 2009b) or deuteron (Afanasiev *et al.*, 2011; Moskal and Smyrski, 2010) beams gave hints for possible  $\eta$  mesic bound states but no clear signal (Kelkar *et al.*, 2013; Metag *et al.*, 2017). New COSY searches have focused on possible  $\eta$  bound states in  $^3\text{He}$  and  $^4\text{He}$  (Adlarson *et al.*, 2013, 2017b). Eta bound states in helium require a large  $\eta$ -nucleon scattering length with real part greater than about 0.7–1.1 fm (Barnea *et al.*, 2017a,b; Fix and Kolesnikov, 2017). At J-PARC the search for  $\eta$ -mesic nuclei is planned using pion induced reactions on  $^7\text{Li}$  and  $^{12}\text{C}$  targets (Fujioka, 2010). Recent measurements of  $\eta'$  photoproduction from nuclear targets

have been interpreted to mean a small  $\eta'$  width in nuclei  $20 \pm 5.0$  MeV at nuclear matter density  $\rho_0$  (Nanova *et al.*, 2012) that might give rise to relatively narrow bound  $\eta'$ -nucleus states accessible to experiments. New experimental groups are looking for possible  $\eta'$  bound states in carbon using the (p, d) reaction at GSI/FAIR (Tanaka *et al.*, 2016, 2018), and photoproduction studies at Spring-8 with carbon and copper (Shimizu, 2017). Exciting possibilities could also be explored at ELSA in Bonn (Metag, 2015). For clean observation of a bound state one needs larger attraction than absorption and thus the real part of the meson-nucleus optical potential to be much bigger than the imaginary part.

### A. The $\eta'$ in medium

The  $\eta'$ -nucleus optical potential has been measured by the CBELSA/TAPS Collaboration in Bonn through studies of excitation functions in photoproduction experiments from nuclear targets. In photoproduction experiments the production cross section is enhanced with the lower effective meson mass in the nuclear medium. When the meson leaves the nucleus it returns on-shell to its free mass with the energy budget conserved at the expense of the kinetic energy so that excitation functions and momentum distributions can provide essential clues to the meson properties in medium (Metag *et al.*, 2012; Weil *et al.*, 2013).

Using this physics a first (indirect) estimate of the  $\eta'$  mass shift has recently been deduced by the CBELSA/TAPS Collaboration (Nanova *et al.*, 2013). The  $\eta'$ -nucleus optical potential  $V_{\text{opt}} = V_{\text{real}} + iW$  deduced from these photoproduction experiments with a carbon target is

$$\begin{aligned} V_{\text{real}}(\rho_0) &= m^* - m = -37 \pm 10 \pm 10 \text{ MeV} \\ W(\rho_0) &= -10 \pm 2.5 \text{ MeV} \end{aligned} \quad (43)$$

at nuclear matter density  $\rho_0$ . In this experiment the average momentum of the produced  $\eta'$  was 1.1 GeV. The experiment was repeated with a niobium target with results  $V_{\text{real}}(\rho_0) = -41 \pm 10 \pm 15$  MeV and  $W(\rho_0) = -13 \pm 3 \pm 3$  MeV (Friedrich *et al.*, 2016; Nanova *et al.*, 2016). This optical potential corresponds to an effective scattering length in medium with real part about 0.5 fm in mean field approximation (switching off the Ericson-Ericson rescattering denominator in Eq. (42)), consistent with the COSY-11 and photoproduction values, Eqs. (38,39). These numbers with small width in medium suggest that bound states may be within reach of forthcoming experiments.

The transparency of nuclei to propagating mesons is illustrated through Fig. 6. Here the cross sections for meson production are parametrized by

$$\sigma(A) = \sigma_0 A^{\alpha(T)} \quad (44)$$



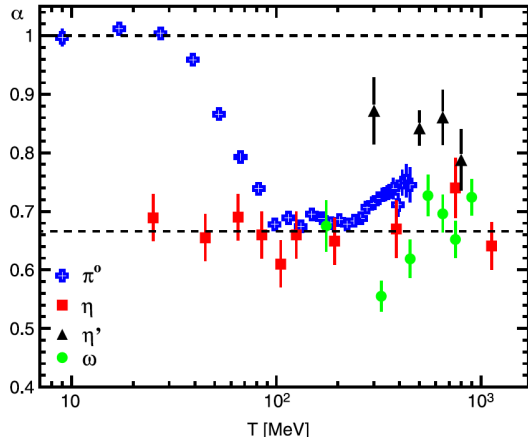


FIG. 6 Dependence of the parameter  $\alpha$  (Eq. (44)) on the kinetic energy  $T$  of the mesons for  $\pi^0$ ,  $\eta$ ,  $\omega$  and  $\eta'$ . The Figure is taken from Nanova *et al.* (2012).

where  $\sigma_0$  is the photoproduction cross-section from a free nucleon and  $\alpha$  is a parameter depending on the meson and its kinetic energy. The value  $\alpha \approx 1$  implies no absorption while  $\alpha \approx \frac{2}{3}$  corresponds to the meson being emitted only from the nuclear surface and thus strong absorption inside the nucleus. Fig. 6 shows that the nucleus is approximately transparent to low-energy pions up to the threshold for  $\Delta$  resonance excitation when  $\alpha$  drops to around  $2/3$ , rising slightly at higher energies. The  $\eta$  and  $\omega$  mesons have strong absorption. For the  $\eta'$  one finds  $\alpha \approx 0.84 \pm 0.03$  averaged over all kinetic energies signifying weaker interaction with the nucleus.

The mass shift, Eq. (43), is very similar to the expectations of the Quark Meson Coupling model, QMC (Bass and Thomas, 2006). In the QMC model medium modifications are calculated at the quark level through coupling of the light quarks in the hadron to the scalar isoscalar  $\sigma$  (and also  $\omega$  and  $\rho$ ) mean fields in the nucleus, for a review see Guichon (1988), Guichon *et al.* (1996) and Saito *et al.* (2007). One works in mean field approximation. The coupling constants for the coupling of light-quarks to the  $\sigma$  (and  $\omega$  and  $\rho$ ) mean fields in the nucleus are adjusted to fit the saturation energy and density of symmetric nuclear matter and the bulk symmetry energy. The large  $\eta$  and  $\eta'$  masses are used to motivate taking a MIT Bag description for the meson wavefunctions, (Tsushima, 2000; Tsushima *et al.*, 1998). Phenomenologically, the MIT Bag gives a good fit to meson properties in free space for the kaons and heavier hadrons (DeGrand *et al.*, 1975). Gluonic topological effects are understood to be “frozen in”, meaning that they are only present implicitly through the masses and mixing angle in the model. The strange-quark component of the wavefunction does not couple to the  $\sigma$  mean field and  $\eta$ - $\eta'$  mixing is readily built into the model. Possible binding energies and the in-medium masses of the  $\eta$  and  $\eta'$  are sensitive to the

flavor-singlet component in the mesons and hence to the non-perturbative glue associated with axial U(1) dynamics (Bass and Thomas, 2006). Working with the mixing scheme in Eq. (13) with an  $\eta$ - $\eta'$  mixing angle of  $-20^\circ$  the QMC prediction for the  $\eta'$  mass in medium at nuclear matter density is 921 MeV, that is a mass shift of  $-37$  MeV. This value is in excellent agreement with the mass shift  $-37 \pm 10 \pm 10$  MeV deduced from photoproduction data, Eq. (43). Mixing increases the octet relative to singlet component in the  $\eta'$ , reducing the binding through increased strange quark component in the  $\eta'$  wavefunction. Without the gluonic mass contribution the  $\eta'$  would be a strange quark state after  $\eta$ - $\eta'$  mixing. Within the QMC model there would be no coupling to the  $\sigma$  mean field and no mass shift so that any observed mass shift is induced by glue associated with the QCD axial anomaly that generates part of the  $\eta'$  mass. For the  $\eta$  meson the potential depth predicted by QMC is  $\approx -100$  MeV at nuclear matter density with  $-20$  degrees mixing. For a pure octet  $\eta$  the model predicts a mass shift of  $\approx -50$  MeV. Increasing the flavor-singlet component in the  $\eta$  at the expense of the octet component gives more attraction, more binding and a larger value of the  $\eta$ -nucleon scattering length,  $a_{\eta N}$ .

In QMC  $\eta$ - $\eta'$  mixing with the phenomenological mixing angle  $-20^\circ$  leads to a factor of two increase in the mass-shift and in the scattering length obtained in the model relative to the prediction for a pure octet  $\eta_8$  (Bass and Thomas, 2006). This result may explain why values of  $a_{\eta N}$  extracted from phenomenological fits to experimental data where the  $\eta$ - $\eta'$  mixing angle is unconstrained give larger values (with real part about 0.9 fm) than those predicted in theoretical coupled-channel models where the  $\eta$  is treated as a pure octet state; see Section V.

Recent coupled-channel model calculations have appeared with mixing and vector meson channels included, with predictions for  $\eta'$  bound states for a range of possible values of  $a_{\eta' N}$  (Nagahiro *et al.*, 2012). Larger mass shifts, downwards by up to 80-150 MeV, were found in Nambu-Jona-Lasinio model calculations (without confinement) (Nagahiro *et al.*, 2006) and in linear sigma model calculations (in a hadronic basis) (Sakai and Jido, 2013) which also gave a rising  $\eta$  effective mass at finite density. Different QCD inspired models of the  $\eta$  and  $\eta'$  nucleus systems are constructed with different selections of “good physics input”: how they treat confinement, chiral symmetry and axial U(1) dynamics. These different theoretical results raise interesting questions about the role of confinement and how massive light pseudoscalar states can be for their wavefunctions to be treated as pure Goldstone bosons in the models.

Experiments in heavy-ion collisions (Averbeck *et al.*, 1997) and  $\eta$  photoproduction from nuclei (Roebig-Landau *et al.*, 1996; Yorita *et al.*, 2000) suggest little modification of the  $N^*(1535)$  excitation in-medium, though some evidence for the broadening of the  $N^*(1535)$

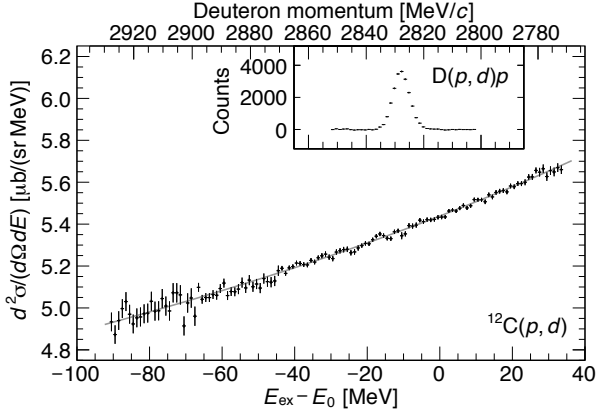


FIG. 7 Excitation spectrum of  $^{11}\text{C}$  measured in the  $^{12}\text{C}(p,d)$  reaction at a proton energy of 2.5 GeV. The horizontal axis is the excitation energy  $E_{\text{ex}}$  referring to the  $\eta'$  emission threshold  $E_0 = 957.78$  MeV. The gray solid curve displays a fit with a third-order polynomial. The inset displays a momentum spectrum of the deuterons in the calibration  $D(p, d)p$  reaction at 1.6 GeV. The Figure is taken from Tanaka *et al.* (2016, 2017).

in nuclei was reported in Yorita *et al.* (2000). In the QMC model the excitation energy is  $\sim 1544$  MeV, consistent with observations, with the scalar attraction compensated by repulsion from coupling to the  $\omega$  mean field (Bass and Thomas, 2006). The QMC model predictions for the kaon and proton mass shifts are a reduction in the  $K^-$  mass of about 100 MeV and effective proton mass about 755 MeV at nuclear matter density (Saito *et al.*, 2007).

The first experiments to search for possible  $\eta'$  bound states in carbon have been performed at GSI with inclusive measurement of the  $^{12}\text{C}(p,d)$  reaction (Tanaka *et al.*, 2016, 2018); see Fig. 7. These experiments exclude very deeply bound narrow states corresponding to real part of the optical potential larger than about 150 MeV predicted (Nagahiro *et al.*, 2013, 2006) based on the NJL model when assuming the  $\eta'$  absorption (imaginary part of the potential of -10 MeV) deduced from measurements of the transparency in nuclei, Eq. (44) (Friedrich *et al.*, 2016; Nanova *et al.*, 2012). More precise studies are planned using semi-inclusive and exclusive measurements with the registration of the decay products of the mesic state (Tanaka *et al.*, 2017).

## B. $\eta$ mesic nuclei

Hints for possible  $\eta$  helium bound states are inferred from observed strong interaction in the  $\eta$  helium system. One finds a sharp rise in the cross section at threshold for  $\eta$  production in both photoproduction from  $^3\text{He}$  and in the proton-deuteron reaction  $dp \rightarrow ^3\text{He} \eta$ , which may hint at a reduced  $\eta$  effective mass in the nuclear medium.

For these data see Fig. 8 and Fig. 9 respectively. One also finds a small and constant value of the analyzing power (Papenbrock *et al.*, 2014) as well as strong variation of the angular asymmetry for  $\eta$  meson emission (Mersmann *et al.*, 2007; Smyrski *et al.*, 2007) indicating strong changes of the phase of the  $s$ -wave production amplitude with energy, as expected with a bound or virtual  $^3\text{He} - \eta$  state (Wilkin *et al.*, 2007). Sharp but less steep rise in the cross section is also seen in the  $dd \rightarrow ^4\text{He} \eta$  reaction (Budzanowski *et al.*, 2009a; Frascaria *et al.*, 1994; Willis *et al.*, 1997; Wronska *et al.*, 2005).

Searches for  $\eta$  mesic nuclei are ongoing with data from the WASA-at-COSY experiment. The focus has so far been on the reaction  $dd \rightarrow ^3\text{He} N \pi$ , in particular studies of the excitation function around the threshold for  $dd \rightarrow ^4\text{He} \eta$ . These excitation functions did not reveal a structure that could be interpreted as a narrow mesic nucleus. Upper limits for the total cross sections for bound state production and decay in the processes  $dd \rightarrow (^4\text{He} - \eta)_{\text{bound}} \rightarrow ^3\text{He} n \pi^0$  and  $dd \rightarrow (^4\text{He} - \eta)_{\text{bound}} \rightarrow ^3\text{He} p \pi^-$  were determined assuming the mesic bound state width lies in the range 5 – 50 MeV. Taking into account recent results on the  $N^*(1535)$  momentum distribution in the  $N^* - ^3\text{He}$  nucleus (Kelkar, 2016; Kelkar *et al.*, 2016), the latest upper limits are about 5 nb and 10 nb for the  $n \pi^0$  and  $p \pi^-$  channels respectively (Adlarson *et al.*, 2017b). These upper limits can be compared to model predictions. For example, within the optical model of Ikeno *et al.* (2017) most of the model parameter space is excluded allowing values of the real and imaginary parts of the potential only between zero and about -60 MeV and -7 MeV respec-

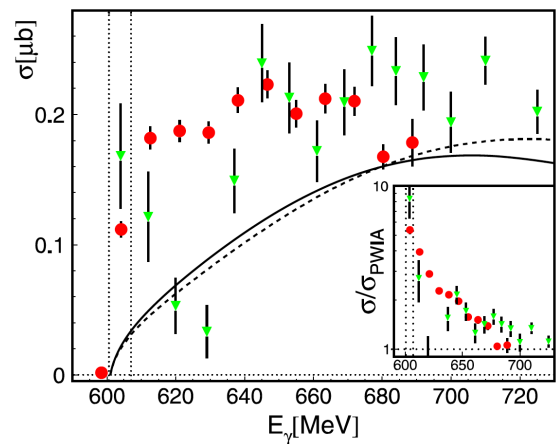


FIG. 8 Total cross section for the  $^3\text{He} \rightarrow ^3\text{He}$  reaction. Data are from references (Pheron *et al.*, 2012) (red points) and (Pfeiffer *et al.*, 2004) (green triangles). Solid (dashed) curves represent plane wave impulse approximation (PWIA) calculations with a realistic (isotropic) angular distribution for the  $\gamma n \rightarrow n \eta$  reaction. Inset: ratio of measured and PWIA cross sections. The Figure is taken from Pheron *et al.* (2012).

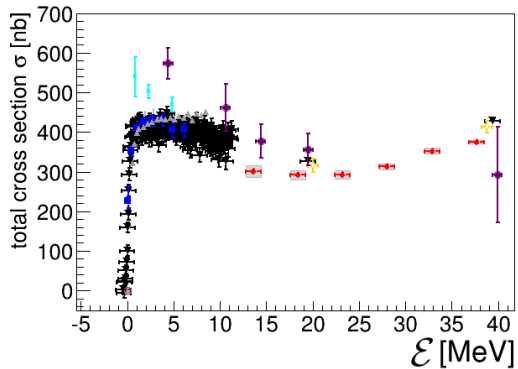


FIG. 9 World data on the  $pd \rightarrow {}^3\text{He}\eta$  reaction close-to-threshold (Adam *et al.*, 2007; Adlarson *et al.*, 2014a, 2018c; Berger *et al.*, 1988; Betigeri *et al.*, 2000; Bilger *et al.*, 2002; Mayer *et al.*, 1996; Mersmann *et al.*, 2007; Rausmann *et al.*, 2009; Smyrski *et al.*, 2007). Notice the sharp rise at threshold. The Figure is adapted from Adlarson *et al.* (2018c).

tively (Skurzok *et al.*, 2018). While the achieved experimental sensitivity of a few nanobarns is too small to make definite conclusions about the existence of a  ${}^4\text{He}\text{-}\eta$  bound state, the situation with  ${}^3\text{He}$  may be more positive. The measurements have similar accuracy of order a few nanobarns with the expected bound state production cross sections for  $pd \rightarrow ({}^3\text{He} - \eta)_{\text{bound}}$  (Wilkin, 2014) expected to be more than 20 times larger than for  $dd \rightarrow ({}^4\text{He} - \eta)_{\text{bound}}$  (Wycech and Krzemień, 2014). Data analysis for the  $pd$  reaction is ongoing (Rundel *et al.*, 2017). Recent calculations in the framework of optical potential (Xie *et al.*, 2017), multi-body calculations (Barnea *et al.*, 2017b), and pionless effective field theory (Barnea *et al.*, 2017a) suggest a possible  ${}^3\text{He}\text{-}\eta$  bound state.

### C. The $\eta'$ at finite temperature

In addition to finite density, axial U(1) symmetry is also expected to be (partially) restored at finite temperature (Kapusta *et al.*, 1996). This result is observed in recent QCD lattice calculations (Bazavov *et al.*, 2012; Cossu *et al.*, 2013; Tomiya *et al.*, 2017). Experimentally, there are hints in RHIC data from relativistic heavy ion collisions for a possible  $\eta'$  mass suppression at finite temperature, with claims of at least -200 MeV mass shift deduced from studies of the intercept  $\lambda$  measured in two-charged-pion Bose-Einstein correlations (Csorgo *et al.*, 2010; Vertesi *et al.*, 2011). With decreasing  $\eta'$  mass one expects a drop in this parameter at small transverse momentum (Vance *et al.*, 1998). The  $\lambda$  parameter accounts for the fact that not all pion pairs are correlated, *e.g.*, as daughters of long-lived strongly decaying resonances and effects from the source dynamics. A key issue in the analysis here is the matching of this dilution factor

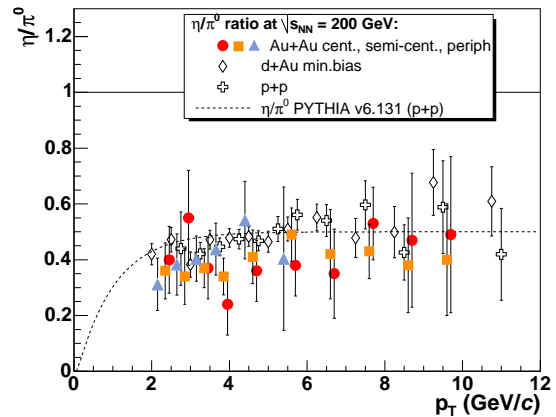


FIG. 10 Ratio of  $\eta$  to  $\pi^0$  production in RHIC PHENIX data. The Figure is taken from Adler *et al.* (2006).

between experiment and theory. The ALICE Collaboration at CERN see similar effects in the data to the RHIC experiments with  $\lambda$  falling by  $\sim 70\%$  at the smallest transverse momentum without attempting an  $\eta'$  mass shift extraction (Adam *et al.*, 2016).

## VII. HIGH-ENERGY $\eta$ AND $\eta'$ PRODUCTION

In higher energy experiments with proton-proton collisions at 450 GeV, or center of mass energy of 28 GeV, the WA102 Collaboration at CERN observed that central production of  $\eta$  and  $\eta'$  mesons seems to have a similar production mechanism which differs from that of the  $\pi^0$  (Barberis *et al.*, 1998). This result has been interpreted in terms of gluonic pomeron-pomeron and pomeron-Reggeon fusion (Close and Schuler, 1999; Lebedowicz *et al.*, 2014). The pomeron is a non-perturbative color-singlet combination of gluon exchange which governs the high energy behavior of hadron scattering processes. Reggeons involve the sum over meson-like exchanges carrying particular quantum numbers in these reactions (Collins and Martin, 1984; Landshoff, 1994).

Semi-inclusive  $\eta$  production in high-energy collisions has been a topical issue since the pioneering work of Field and Feynman (1977). One finds the interesting result that the ratio of  $\eta$  to  $\pi^0$  production rises rapidly with the transverse momentum  $p_t$  of the produced meson and levels off at at  $R_{\eta/\pi^0} \sim 0.4 - 0.5$  above  $p_t \sim 2$  GeV in nuclear collisions (proton-proton, proton-nucleus and nucleus-nucleus) independent of the colliding nuclei; see Fig. 10. These results hold over a wide range of center-of-mass energy ( $\sqrt{s_{NN}} \sim 30 - 8000$  GeV) as well as meson production carrying momentum fraction  $x_p > 0.35$  of the exchanged photon in electron positron collisions at LEP,  $\sqrt{s} = 91.2$  GeV.

In these relativistic heavy-ion collisions the invariant

yields per nucleon-nucleon collision are increasingly depleted with centrality in comparison to proton-proton results at the same center-of-mass energy. The maximum suppression factor is about 5 in central Au+Au collisions (Adler *et al.*, 2006). The measured  $\eta/\pi^0$  ratio is independent of both the reaction centrality as well as the species of colliding protons or nuclei. These results indicate that any initial and/or final state nuclear effects influence the production of light neutral mesons at large  $p_t$  in the same way. The approximately constant ratio for  $\eta$  to  $\pi^0$  production indicates that the parent quark or gluon parton first loses energy in the dense medium of the collision and then fragments into leading mesons  $\eta$  and  $\pi^0$  in the vacuum according to the same probabilities that govern high  $p_t$  hadron production in more elementary  $e^+e^-$  and proton-proton collisions. These results observed at RHIC in PHENIX (Adler *et al.*, 2006, 2007) and STAR (Abelev *et al.*, 2010) data at  $\sqrt{s_{NN}} = 200$  GeV are also observed by ALICE at the LHC up to 8 TeV (Acharya *et al.*, 2018a,b,c), with earlier measurements summarized in Adler *et al.* (2007).

The fragmentation functions for  $\eta$  production in high energy processes are discussed in Aidala *et al.* (2011). First measurements of  $\eta'$  production in proton-proton collisions at center of mass energy 200 GeV are reported by the PHENIX Collaboration in Adare *et al.* (2011b). In ALEPH data from LEP  $\eta'$  production was observed to be anomalously suppressed compared to the expectations of string fragmentation models without an additional “ $\eta'$  suppression factor”, possibly associated with the mass of the produced  $\eta'$  (Barate *et al.*, 2000). The cross section and double helicity asymmetry for  $\eta$  production is studied by PHENIX at midrapidity with comparison to  $\pi^0$  production in Adare *et al.* (2011a). The transverse single-spin asymmetry for forward  $\eta$  production looks as large as if not larger than that for forward  $\pi^0$  production – see PHENIX (Adare *et al.*, 2014) and STAR (Adamczyk *et al.*, 2012) – and may be related to quark-gluon correlation functions.

### A. $\eta'$ - $\pi$ interactions and $1^{-+}$ exotics

Following the discussion in Section II, the OZI-violating interaction  $\xi Q^2 \partial_\mu \pi_a \partial^\mu \pi_a$  gives a potentially important tree-level contribution to the decay  $\eta' \rightarrow \eta \pi \pi$  (Di Vecchia *et al.*, 1981). Suppose one takes  $\xi$  as negative with attractive interaction. When iterated in the Bethe-Salpeter equation for  $\eta'\pi$  rescattering this interaction then yields a dynamically generated resonance with quantum numbers  $J^{PC} = 1^{-+}$  and mass about 1400 MeV. The dynamics here is mediated by the singlet OZI-violating coupling of the  $\eta'$  (Bass and Marco, 2002). One finds a possible dynamical interpretation of light-mass  $1^{-+}$  exotic states, *e.g.*, as observed in experiments at BNL (Adams *et al.*, 1998; Chung *et al.*, 1999; Ivanov

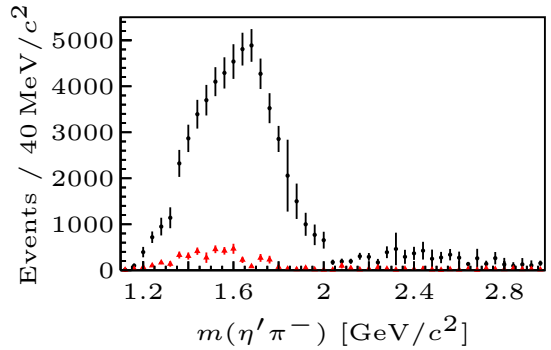


FIG. 11 The  $\eta'\pi^-$  exotic partial wave  $1^{-+}$  (upper data) is much enhanced compared to  $\eta\pi^-$  (lower data) in exclusive production from 191 GeV  $\pi^-$  scattering on a hydrogen fixed target. The Figure is taken from Adolph *et al.* (2015).

*et al.*, 2001; Thompson *et al.*, 1997) and CERN (Abele *et al.*, 1998), see also Szczepaniak *et al.* (2003). This OZI-violating interaction will also contribute to higher  $L$  odd partial waves with quantum numbers  $L^{-+}$ . These states are particularly interesting because the quantum numbers  $1^{-+}, 3^{-+}, 5^{-+}, \dots$  are inconsistent with a simple quark-antiquark bound state. The COMPASS experiment at CERN has recently measured exclusive production of  $\eta'\pi^-$  and  $\eta\pi^-$  in 191 GeV  $\pi^-$  collisions on a hydrogen target (Adolph *et al.*, 2015). They find the interesting result that  $\eta'\pi^-$  production is enhanced relative to  $\eta\pi^-$  production by a factor of 5-10 in the exotic  $L = 1, 3, 5$  partial waves with quantum numbers  $L^{-+}$  in the inspected invariant mass range up to 3 GeV; see Fig. 11. No enhancement was observed in the even  $L$  partial waves. For further recent discussion, see also Rodas *et al.* (2017).

Glueballs, postulated bound states of gluons with integer spin, may also couple strongly to the  $\eta'$  and  $\eta$ . Glueball states are found in lattice pure glue theory with mixing with quark-antiquark mesons induced in full QCD (Gregory *et al.*, 2012a; Gui *et al.*, 2013; Morningstar and Peardon, 1999; Sun *et al.*, 2017). The lightest glueball state is expected to be a scalar with the prime candidates discussed in the literature being the  $f_0(1500)$  and  $f_0(1710)$  states, much heavier than the lightest mass quark-antiquark state – the pseudoscalar pion. We refer to Frere and Heeck (2015) and Brunner and Rebhan (2015) for recent discussion of scalar glueball decays to  $\eta$  and  $\eta'$  final states. Particularly interesting is a pseudoscalar glueball in the mass range 2-3 GeV where recent calculations suggest a narrow state and very restricted decay pattern involving  $\eta$  or  $\eta'$  mesons that can be searched for in central exclusive production experiments, *e.g.*, at the LHC (Brunner and Rebhan, 2017).

## VIII. SUMMARY AND FUTURE CHALLENGES

The isoscalar  $\eta$  and  $\eta'$  mesons are sensitive to the interface of chiral and non-perturbative dynamics. One finds a rich phenomenology involving OZI-violation, meson production dynamics from threshold through to high-energy collisions and the coupling to new excited nucleon resonances. Axial U(1) symmetry is expected to be partially restored in QCD media at finite densities and temperature. This, in turn, leads to predictions for the  $\eta$  and  $\eta'$  effective mass shifts in medium and possible meson bound states in nuclei. The non-perturbative glue which generates the large  $\eta$  and  $\eta'$  masses also has the potential to induce strong CP violation in the neutron electric dipole moment which is not observed. A possible solution to this strong CP puzzle is connected with a new axion particle which, if it exists, might also be associated with dark matter. Understanding the  $\eta$  and  $\eta'$  systems is important to nuclear, high-energy and astrophysics.

New experiments will give valuable insight into  $\eta$  and  $\eta'$  physics. The search for  $\eta$  and  $\eta'$  mesic nuclei will help pin down the dynamics of axial U(1) symmetry breaking in low-energy QCD. Determining the  $\eta'$  properties at finite temperature in relativistic heavy-ion collisions would further probe axial U(1) dynamics in the QCD phase diagram. Precision studies of  $\eta$  and  $\eta'$  decays are a probe for new physics beyond the Standard Model. Production of  $\eta'$  mesons in connection with glueball production will test theoretical ideas about gluonic excitations in non-perturbative QCD.

## ACKNOWLEDGMENTS

We thank C. Aidala, V. Burkert, M. Faessler, A. Fix, S. Hirenzaki, K. Itahashi, J. Krzysiak, W. Melnitchouk, V. Metag, G. Moskal, E. Oset, M. Pitschmann, A. Rebhan, H. Shimizu, M. Silarski, M. Skurzok, Y. Tanaka, A. W. Thomas and M. Weber for helpful discussions. We acknowledge support from the Polish National Science Centre through the grant No. 2016/23/B/ST2/00784 and the Foundation for Polish Science through the TEAM/2017-4/39 programme.

## REFERENCES

- Abdel-Bary, M., *et al.* (TOF) (2003), Eur. Phys. J. **A16**, 127  
Abel, C., *et al.* (2017), Phys. Rev. **X7** (4), 041034  
Abele, A., *et al.* (Crystal Barrel) (1998), Phys. Lett. **B423**, 175  
Abelev, B. I., *et al.* (STAR) (2010), Phys. Rev. **C81**, 064904  
Ablikim, M., *et al.* (BESIII) (2015a), Phys. Rev. **D92**, 012014  
Ablikim, M., *et al.* (BESIII) (2015b), Phys. Rev. **D92** (1), 012001  
Ablikim, M., *et al.* (BESIII) (2017), Phys. Rev. Lett. **118** (1), 012001  
Accardi, A., *et al.* (2016), Eur. Phys. J. **A52** (9), 268  
Acharya, S., *et al.* (ALICE) (2018a), Phys. Rev. **C98** (4), 044901  
Acharya, S., *et al.* (ALICE) (2018b), Eur. Phys. J. **C78** (8), 624  
Acharya, S., *et al.* (ALICE) (2018c), Eur. Phys. J. **C78** (3), 263  
Adachi, I., *et al.* (Belle) (2008), Phys. Lett. **B662**, 323  
Adam, H. H., *et al.* (COSY-11) (2007), Phys. Rev. **C75**, 014004  
Adam, J., *et al.* (ALICE) (2016), Phys. Rev. **C93** (2), 024905  
Adamczyk, L., *et al.* (STAR) (2012), Phys. Rev. **D86**, 051101  
Adams, G. S., *et al.* (E852) (1998), Phys. Rev. Lett. **81**, 5760  
Adare, A., *et al.* (PHENIX) (2011a), Phys. Rev. **D83**, 032001  
Adare, A., *et al.* (PHENIX) (2011b), Phys. Rev. **D83**, 052004  
Adare, A., *et al.* (PHENIX) (2014), Phys. Rev. **D90** (7), 072008  
Adlarson, P., *et al.* (WASA-at-COSY) (2012), Phys. Lett. **B707**, 243  
Adlarson, P., *et al.* (WASA-at-COSY) (2013), Phys. Rev. **C87** (3), 035204  
Adlarson, P., *et al.* (WASA-at-COSY) (2014a), Eur. Phys. J. **A50**, 100  
Adlarson, P., *et al.* (WASA-at-COSY) (2014b), Phys. Rev. **C90** (4), 045207  
Adlarson, P., *et al.* (WASA-at-COSY) (2016), Phys. Rev. **C94** (6), 065206  
Adlarson, P., *et al.* (A2) (2017a), Phys. Rev. **C95** (3), 035208  
Adlarson, P., *et al.* (WASA-at-COSY) (2017b), Nucl. Phys. **A959**, 102  
Adlarson, P., *et al.* (WASA-at-COSY) (2018a), Phys. Lett. **B784**, 378  
Adlarson, P., *et al.* (WASA-at-COSY) (2018b), Phys. Rev. Lett. **120** (2), 022002  
Adlarson, P., *et al.* (WASA-at-COSY) (2018c), Phys. Lett. **B782**, 297  
Adler, S. L. (1969), Phys. Rev. **177**, 2426  
Adler, S. S., *et al.* (PHENIX) (2006), Phys. Rev. Lett. **96**, 202301  
Adler, S. S., *et al.* (PHENIX) (2007), Phys. Rev. **C75**, 024909  
Adolph, C., *et al.* (WASA-at-COSY) (2009), Phys. Lett. **B677**, 24  
Adolph, C., *et al.* (COMPASS) (2015), Phys. Lett. **B740**, 303  
Afanasyev, S. V., *et al.* (2011), Phys. Part. Nucl. Lett. **8**, 1073  
Aidala, C. A., S. D. Bass, D. Hasch, and G. K. Mallot (2013), Rev. Mod. Phys. **85**, 655  
Aidala, C. A., F. Ellinghaus, R. Sassot, J. P. Seele, and M. Stratmann (2011), Phys. Rev. **D83**, 034002  
Al Ghouli, H., *et al.* (GlueX) (2017), Phys. Rev. **C95** (4), 042201  
Altarelli, G. (2013), arXiv:1303.2842 [hep-ph]  
Ambrosino, F., *et al.* (KLOE) (2007), Phys. Lett. **B648**, 267  
Ambrosino, F., *et al.* (KLOE) (2009), JHEP **07**, 105  
Ambrosino, F., *et al.* (KLOE-2) (2011), Phys. Lett. **B694**, 16  
del Amo Sanchez, P., *et al.* (BaBar) (2011), Phys. Rev. **D84**, 052001  
Anastasi, A., *et al.* (KLOE-2) (2016), JHEP **05**, 019  
Anisovich, A. V., V. Burkert, P. M. Collins, M. Dugger, E. Klempt, V. A. Nikonov, B. G. Ritchie, A. V. Sarantsev, and U. Thoma (2017), Phys. Lett. **B772**, 247  
Anisovich, A. V., V. Burkert, M. Dugger, E. Klempt, V. A. Nikonov, B. G. Ritchie, A. V. Sarantsev, and U. Thoma (2018), Phys. Lett. **B785**, 626  
Anisovich, A. V., E. Klempt, B. Krusche, V. A. Nikonov, A. V. Sarantsev, U. Thoma, and D. Werthmueller (2015),



- Eur. Phys. J. **A51** (6), 72
- Aoki, S., *et al.* (2017), Eur. Phys. J. **C77** (2), 112
- Armstrong, C. S., *et al.* (Jefferson Lab E94014) (1999), Phys. Rev. **D60**, 052004
- Arnaldi, R., *et al.* (NA60) (2009), Phys. Lett. **B677**, 260
- Arndt, R. A., W. J. Briscoe, T. W. Morrison, I. I. Strakovsky, R. L. Workman, and A. B. Gridnev (2005), Phys. Rev. **C72**, 045202
- Atwood, D., and A. Soni (1997), Phys. Lett. **B405**, 150
- Aubert, B., *et al.* (BaBar) (2001), arXiv:hep-ex/0109034 [hep-ex]
- Averbeck, R., *et al.* (TAPS) (1997), Z. Phys. **A359**, 65
- Aznauryan, I. G., and V. D. Burkert (2012), Prog. Part. Nucl. Phys. **67**, 1
- Babusci, D., *et al.* (KLOE-2) (2013a), JHEP **01**, 119
- Babusci, D., *et al.* (KLOE-2) (2013b), Phys. Lett. **B718**, 910
- Balestra, F., *et al.* (DISTO) (2000), Phys. Lett. **B491**, 29
- Bali, G., S. Collins, and J. Simeth (2018), EPJ Web Conf. **175**, 05028
- Bali, G. S., S. Collins, S. Drr, and I. Kanamori (2015), Phys. Rev. **D91** (1), 014503
- Ball, P., J. M. Frere, and M. Tytgat (1996), Phys. Lett. **B365**, 367
- Barate, R., *et al.* (ALEPH) (2000), Eur. Phys. J. **C16**, 613
- Barberis, D., *et al.* (WA102) (1998), Phys. Lett. **B427**, 398
- Barnea, N., B. Bazak, E. Friedman, and A. Gal (2017a), Phys. Lett. **B771**, 297, [Erratum: Phys. Lett. **B775**, 364 (2017)]
- Barnea, N., E. Friedman, and A. Gal (2017b), Nucl. Phys. **A968**, 35
- Barth, R., *et al.* (KaoS) (1997), Phys. Rev. Lett. **78**, 4007
- Baskov, V. A., *et al.* (2012), PoS **Baldin-ISHEPP-XXI**, 102
- Bass, S. D. (1999), Phys. Lett. **B463**, 286
- Bass, S. D. (2000), arXiv:hep-ph/0006348 [hep-ph]
- Bass, S. D. (2005), Rev. Mod. Phys. **77**, 1257
- Bass, S. D. (2009), Acta Phys. Polon. Supp. **2**, 11
- Bass, S. D., and E. Marco (2002), Phys. Rev. **D65**, 057503
- Bass, S. D., and A. W. Thomas (2006), Phys. Lett. **B634**, 368
- Bass, S. D., and A. W. Thomas (2010), Phys. Lett. **B684**, 216
- Bass, S. D., and A. W. Thomas (2014), Acta Phys. Polon. **B45**, 627
- Baudis, L. (2018), arXiv:1801.08128 [astro-ph.CO]
- Baur, R., J. Kambor, and D. Wyler (1996), Nucl. Phys. **B460**, 127
- Bazavov, A., *et al.* (HotQCD) (2012), Phys. Rev. **D86**, 094503
- Behrend, H. J., *et al.* (CELLO) (1991), Z. Phys. **C49**, 401
- Behrens, B. H., *et al.* (CLEO) (1998), Phys. Rev. Lett. **80**, 3710
- Bell, J. S., and R. Jackiw (1969), Nuovo Cim. **A60**, 47
- Bennett, G. W., *et al.* (Muon g-2) (2006), Phys. Rev. **D73**, 072003
- Bergdolt, A. M., *et al.* (1993), Phys. Rev. **D48**, 2969
- Berger, J., *et al.* (SPES4) (1988), Phys. Rev. Lett. **61**, 919
- Betigeri, M., *et al.* (GEM) (2000), Phys. Lett. **B472**, 267
- Bijnens, J., G. Faldt, and B. M. K. Nefkens (2002), *Production, interaction and decay of the eta meson. Proceedings, Workshop, Uppsala, Sweden, October 25-27, 2001*, [Phys. Scripta **T99**, pp.1(2002)]
- Bilger, R., *et al.* (WASA/PROMICE) (2002), Phys. Rev. **C65**, 044608
- Braun-Munzinger, P., and J. Wambach (2009), Rev. Mod. Phys. **81**, 1031
- Browder, T. E., *et al.* (CLEO) (1998), Phys. Rev. Lett. **81**, 1786
- Brunner, F., and A. Rebhan (2015), Phys. Rev. **D92** (12), 121902
- Brunner, F., and A. Rebhan (2017), Phys. Lett. **B770**, 124
- Budzanowski, A., *et al.* (GEM) (2009a), Nucl. Phys. **A821**, 193
- Budzanowski, A., *et al.* (GEM) (2009b), Phys. Rev. **C79**, 012201
- Burkert, V. D. (2018), Few Body Syst. **59** (4), 57
- Calen, H., *et al.* (WASA/PROMICE) (1996), Phys. Lett. **B366**, 39
- Calen, H., *et al.* (WASA/PROMICE) (1998), Phys. Rev. **C58**, 2667
- Chiang, W.-T., S. N. Yang, M. Vanderhaeghen, and D. Drechsel (2003), Nucl. Phys. **A723**, 205
- Chiavassa, E., *et al.* (PINOT) (1994), Phys. Lett. **B322**, 270
- Chrien, R. E., *et al.* (1988), Phys. Rev. Lett. **60**, 2595
- Christ, N. H., C. Dawson, T. Izubuchi, C. Jung, Q. Liu, R. D. Mawhinney, C. T. Sachrajda, A. Soni, and R. Zhou (2010), Phys. Rev. Lett. **105**, 241601
- Chung, S. U., *et al.* (E852) (1999), Phys. Rev. **D60**, 092001
- Cichy, K., E. Garcia-Ramos, K. Jansen, K. Ottnad, and C. Urbach (ETM) (2015), JHEP **09**, 020
- Close, F. E. (1979), *An Introduction to Quarks and Partons* (Academic Press/London)
- Close, F. E., and G. A. Schuler (1999), Phys. Lett. **B464**, 279
- Colangelo, G., S. Lanz, H. Leutwyler, and E. Passemar (2017), Phys. Rev. Lett. **118** (2), 022001
- Collins, P., *et al.* (2017), Phys. Lett. **B771**, 213
- Collins, P. D. B., and A. D. Martin (1984), *Hadron Interactions* (Adam Hilger, Bristol U. K.)
- Cossu, G., S. Aoki, H. Fukaya, S. Hashimoto, T. Kaneko, H. Matsufuru, and J.-I. Noaki (2013), Phys. Rev. **D87** (11), 114514, [Erratum: Phys. Rev. **D88**, no.1, 019901 (2013)]
- Crede, V., *et al.* (CBELSA/TAPS) (2009), Phys. Rev. **C80**, 055202
- Crewther, R. J. (1978), Acta Phys. Austriaca Suppl. **19**, 47
- Crewther, R. J., P. Di Vecchia, G. Veneziano, and E. Witten (1979), Phys. Lett. **88B**, 123, [Erratum: Phys. Lett. **91B**, 487 (1980)]
- Csorgo, T., R. Vertesi, and J. Sziklai (2010), Phys. Rev. Lett. **105**, 182301
- Czerwinski, E., P. Moskal, and M. Silarski (COSY-11) (2014a), Acta Phys. Polon. **B45** (3), 739
- Czerwinski, E., *et al.* (COSY-11) (2010), Phys. Rev. Lett. **105**, 122001
- Czerwinski, E., *et al.* (COSY-11) (2014b), Phys. Rev. Lett. **113**, 062004
- Czyzykiewicz, R., *et al.* (COSY-11) (2007), Phys. Rev. Lett. **98**, 122003
- Dalton, M. M., *et al.* (2009), Phys. Rev. **C80**, 015205
- Dashen, R. F. (1969), Phys. Rev. **183**, 1245
- DeGrand, T. A., R. L. Jaffe, K. Johnson, and J. E. Kiskis (1975), Phys. Rev. **D12**, 2060
- Deloff, A. (2004), Phys. Rev. **C69**, 035206
- Deshpande, A. (2017), Int. J. Mod. Phys. **E26** (01n02), 1740007
- Di Donato, C., G. Ricciardi, and I. Bigi (2012), Phys. Rev. **D85**, 013016

- Di Vecchia, P., F. Nicodemi, R. Pettorino, and G. Veneziano (1981), Nucl. Phys. **B181**, 318
- Di Vecchia, P., and G. Veneziano (1980), Nucl. Phys. **B171**, 253
- Dighe, A. S., M. Gronau, and J. L. Rosner (1996), Phys. Lett. **B367**, 357, [Erratum: Phys. Lett. **B377**, 325(1996)]
- Dighe, A. S., M. Gronau, and J. L. Rosner (1997), Phys. Rev. Lett. **79**, 4333
- Dugger, M., *et al.* (CLAS) (2006), Phys. Rev. Lett. **96**, 062001, [Erratum: Phys. Rev. Lett. **96**, 169905(2006)]
- Ellis, J. (2014), Int. J. Mod. Phys. **A29** (31), 1430072
- Ericson, T. E. O., and W. Weise (1988), *Pions and Nuclei* (Clarendon Press, Oxford, UK)
- Escribano, R., and J.-M. Frere (2005), JHEP **06**, 029
- Escribano, R., and J. Nadal (2007), JHEP **05**, 006
- Faeldt, G., and C. Wilkin (1996), Phys. Lett. **B382**, 209
- Faltdt, G., and C. Wilkin (2001), Phys. Scripta **64**, 427
- Fang, S.-s., A. Kupsc, and D.-h. Wei (2018), Chin. Phys. **C42** (4), 042002
- Feldmann, T. (2000), Int. J. Mod. Phys. **A15**, 159
- Feldmann, T., and P. Kroll (1998), Eur. Phys. J. **C5**, 327
- Feldmann, T., P. Kroll, and B. Stech (1998), Phys. Rev. **D58**, 114006
- Field, R. D., and R. P. Feynman (1977), Phys. Rev. **D15**, 2590
- Fix, A., and O. Kolesnikov (2017), Phys. Lett. **B772**, 663
- Frascaria, R., *et al.* (SPES4) (1994), Phys. Rev. **C50** (2), R537
- Frere, J.-M., and J. Heeck (2015), Phys. Rev. **D92** (11), 114035
- Friedrich, S., *et al.* (CBELSA/TAPS) (2016), Eur. Phys. J. **A52** (9), 297
- Fritzsche, H. (1997), Phys. Lett. **B415**, 83
- Fritzsche, H., and P. Minkowski (1975), Nuovo Cim. **A30**, 393
- Fujioka, H. (2010), Acta Phys. Polon. **B41**, 2261
- Garcia-Recio, C., J. Nieves, T. Inoue, and E. Oset (2002), Phys. Lett. **B550**, 47
- Garzon, E. J., and E. Oset (2015), Phys. Rev. **C91** (2), 025201
- Gasser, J., and H. Leutwyler (1982), Phys. Rept. **87**, 77
- Gauzzi, P. (KLOE-2) (2012), J. Phys. Conf. Ser. **349**, 012002
- Gell-Mann, M. (1961), Caltech Report CTSL-20
- Gell-Mann, M., R. J. Oakes, and B. Renner (1968), Phys. Rev. **175**, 2195
- Gell-Mann, M., and K. M. Watson (1954), Ann. Rev. Nucl. Part. Sci. **4**, 219
- Georgi, H. (1984), *Weak Interactions and Modern Particle Theory* (Menlo Park, USA: Benjamin/Cummings)
- Gilman, F. J., and R. Kauffman (1987), Phys. Rev. **D36**, 2761, [Erratum: Phys. Rev. **D37**, 3348(1988)]
- Green, A. M., and S. Wycech (1999), Phys. Rev. **C60**, 035208
- Green, A. M., and S. Wycech (2005), Phys. Rev. **C71**, 014001, [Erratum: Phys. Rev. **C72**, 029902(2005)]
- Greensite, J. (2011), Lect. Notes Phys. **821**, 1
- Gregory, E., A. Irving, B. Lucini, C. McNeile, A. Rago, C. Richards, and E. Rinaldi (2012a), JHEP **10**, 170
- Gregory, E. B., A. C. Irving, C. M. Richards, and C. McNeile (UKQCD) (2012b), Phys. Rev. **D86**, 014504
- Gronberg, J., *et al.* (CLEO) (1998), Phys. Rev. **D57**, 33
- Gui, L.-C., Y. Chen, G. Li, C. Liu, Y.-B. Liu, J.-P. Ma, Y.-B. Yang, and J.-B. Zhang (CLQCD) (2013), Phys. Rev. Lett. **110** (2), 021601
- Guichon, P. A. M. (1988), Phys. Lett. **B200**, 235
- Guichon, P. A. M., K. Saito, E. N. Rodionov, and A. W. Thomas (1996), Nucl. Phys. **A601**, 349
- Guo, P., I. V. Danilkin, C. Fernandez-Ramirez, V. Mathieu, and A. P. Szczepaniak (2017), Phys. Lett. **B771**, 497
- Gyulassy, M., and L. McLerran (2005), Nucl. Phys. **A750**, 30
- Haider, Q., and L. C. Liu (1986), Phys. Lett. **B172**, 257
- Hall, J. M. M., W. Kamleh, D. B. Leinweber, B. J. Menadue, B. J. Owen, A. W. Thomas, and R. D. Young (2015), Phys. Rev. Lett. **114** (13), 132002
- Harland-Lang, L. A., V. A. Khoze, M. G. Ryskin, and W. J. Stirling (2013), Eur. Phys. J. **C73**, 2429
- Hertzog, D. W. (2016), EPJ Web Conf. **118**, 01015
- Hibou, F., *et al.* (SPES3) (1998), Phys. Lett. **B438**, 41
- 't Hooft, G. (1976a), Phys. Rev. **D14**, 3432, [Erratum: Phys. Rev. **D18**, 2199(1978)]
- 't Hooft, G. (1976b), Phys. Rev. Lett. **37**, 8
- Hou, W.-S., and B. Tseng (1998), Phys. Rev. Lett. **80**, 434
- Hyodo, T., D. Jido, and A. Hosaka (2008), Phys. Rev. **C78**, 025203
- Iizuka, J. (1966), Prog. Theor. Phys. Suppl. **37**, 21
- Ikeno, N., H. Nagahiro, D. Jido, and S. Hirenzaki (2017), Eur. Phys. J. **A53** (10), 194
- Inoue, T., and E. Oset (2002), Nucl. Phys. **A710**, 354
- Inoue, T., E. Oset, and M. J. Vicente Vacas (2002), Phys. Rev. **C65**, 035204
- Ioffe, B. L. (2006), Int. J. Mod. Phys. **A21**, 6249
- Isgur, N., and G. Karl (1978), Phys. Rev. **D18**, 4187
- Ivanov, E. I., *et al.* (E852) (2001), Phys. Rev. Lett. **86**, 3977
- Jaegle, I., *et al.* (CBELSA/TAPS) (2011), Eur. Phys. J. **A47**, 11
- Jarlskog, C., and E. Shabalin (2002), Phys. Scripta **T99**, 23
- Jegerlehner, F. (2017), Springer Tracts Mod. Phys. **274**, pp.1
- Kaiser, N., P. B. Siegel, and W. Weise (1995), Phys. Lett. **B362**, 23
- Kambor, J., C. Wiesendanger, and D. Wyler (1996), Nucl. Phys. **B465**, 215
- Kampf, K., M. Knecht, J. Novotny, and M. Zdrahal (2011), Phys. Rev. **D84**, 114015
- Kaptari, L. P., and B. Kampfer (2008), Eur. Phys. J. **A37**, 69
- Kapusta, J. I., D. Kharzeev, and L. D. McLerran (1996), Phys. Rev. **D53**, 5028
- Kashevarov, V. L., *et al.* (A2) (2017), Phys. Rev. Lett. **118** (21), 212001
- Kawarabayashi, K., and N. Ohta (1980), Nucl. Phys. **B175**, 477
- Kawasaki, M., and K. Nakayama (2013), Ann. Rev. Nucl. Part. Sci. **63**, 69
- Kelkar, N. G. (2016), Eur. Phys. J. **A52** (10), 309
- Kelkar, N. G., D. Bedoya Fierro, and P. Moskal (2016), Acta Phys. Polon. **B47**, 299
- Kelkar, N. G., K. P. Khemchandani, N. J. Upadhyay, and B. K. Jain (2013), Rept. Prog. Phys. **76**, 066301
- Khoukaz, A., *et al.* (COSY-11) (2004), Eur. Phys. J. **A20**, 345
- Kienle, P., and T. Yamazaki (2004), Prog. Part. Nucl. Phys. **52**, 85
- Klaja, J., *et al.* (COSY-11) (2010a), Phys. Rev. **C81**, 035209
- Klaja, P., *et al.* (COSY-11) (2010b), Phys. Lett. **B684**, 11
- Klemt, E., and A. Zaitsev (2007), Phys. Rept. **454**, 1
- Kodaira, J. (1980), Nucl. Phys. **B165**, 129
- Kogut, J. B., and L. Susskind (1975), Phys. Rev. **D11**, 3594

- Kroll, P., and K. Passek-Kumericki (2013), *J. Phys.* **G40**, 075005
- Krusche, B. (CBELSA-TAPS, Crystal Barrel/TAPS) (2012), *J. Phys. Conf. Ser.* **349**, 012003
- Krusche, B., and C. Wilkin (2014), *Prog. Part. Nucl. Phys.* **80**, 43
- Kubis, B., and J. Plenler (2015), *Eur. Phys. J.* **C75** (6), 283
- Kupsc, A. (2009), *Int. J. Mod. Phys.* **E18**, 1255
- Landshoff, P. V. (1994), arXiv:hep-ph/9410250 [hep-ph]
- Lattimer, J. M., and M. Prakash (2016), *Phys. Rept.* **621**, 127
- Lebiedowicz, P., O. Nachtmann, and A. Szczurek (2014), *Annals Phys.* **344**, 301
- Lepage, G. P., and S. J. Brodsky (1980), *Phys. Rev.* **D22**, 2157
- Leutwyler, H. (1998), *Nucl. Phys. Proc. Suppl.* **64**, 223
- Leutwyler, H. (2013), *Mod. Phys. Lett.* **A28**, 1360014
- Levi Sandri, P., *et al.* (GrAAL) (2015), *Eur. Phys. J.* **A51** (7), 77
- Liu, Z.-W., W. Kamleh, D. B. Leinweber, F. M. Stokes, A. W. Thomas, and J.-J. Wu (2016), *Phys. Rev. Lett.* **116** (8), 082004
- Mantry, S., M. Pitschmann, and M. J. Ramsey-Musolf (2014), *Phys. Rev.* **D90** (5), 054016
- Mayer, B., *et al.* (SPES2) (1996), *Phys. Rev.* **C53**, 2068
- Mersmann, T., *et al.* (ANKE) (2007), *Phys. Rev. Lett.* **98**, 242301
- Metag, V. (2015), *Hyperfine Interact.* **234** (1-3), 25
- Metag, V., M. Nanova, and E. Ya. Paryev (2017), *Prog. Part. Nucl. Phys.* **97**, 199
- Metag, V., M. Thiel, H. Berghauser, S. Friedrich, B. Lemmer, U. Mosel, and J. Weil (A2) (2012), *Prog. Part. Nucl. Phys.* **67**, 530
- Meyer, H. O., *et al.* (1999), *Phys. Rev. Lett.* **83**, 5439
- Meyer, H. O., *et al.* (2001), *Phys. Rev.* **C63**, 064002
- Michael, C., K. Ottnad, and C. Urbach (ETM) (2013), *Phys. Rev. Lett.* **111** (18), 181602
- Morningstar, C. J., and M. J. Peardon (1999), *Phys. Rev.* **D60**, 034509
- Moskal, P. (2004), arXiv:hep-ph/0408162 [hep-ph]
- Moskal, P., and J. Smyrski (COSY-11) (2010), *Acta Phys. Polon.* **B41**, 2281
- Moskal, P., M. Wolke, A. Khoukaz, and W. Oelert (2002), *Prog. Part. Nucl. Phys.* **49**, 1
- Moskal, P., *et al.* (COSY-11) (1998), *Phys. Rev. Lett.* **80**, 3202
- Moskal, P., *et al.* (COSY-11) (2000a), *Phys. Lett.* **B474**, 416
- Moskal, P., *et al.* (COSY-11) (2000b), *Phys. Lett.* **B482**, 356
- Moskal, P., *et al.* (COSY-11) (2004), *Phys. Rev.* **C69**, 025203
- Moskal, P., *et al.* (COSY-11) (2006), *J. Phys.* **G32**, 629
- Moskal, P., *et al.* (COSY-11) (2009), *Phys. Rev.* **C79**, 015208
- Moskal, P., *et al.* (COSY-11) (2010), *Eur. Phys. J.* **A43**, 131
- Nagahiro, H., S. Hirenzaki, E. Oset, and A. Ramos (2012), *Phys. Lett.* **B709**, 87
- Nagahiro, H., D. Jido, H. Fujioka, K. Itahashi, and S. Hirenzaki (2013), *Phys. Rev.* **C87** (4), 045201
- Nagahiro, H., M. Takizawa, and S. Hirenzaki (2006), *Phys. Rev.* **C74**, 045203
- Nakayama, K., J. Haidenbauer, C. Hanhart, and J. Speth (2003), *Phys. Rev.* **C68**, 045201
- Nanova, M., *et al.* (CBELSA/TAPS) (2012), *Phys. Lett.* **B710**, 600
- Nanova, M., *et al.* (CBELSA/TAPS) (2013), *Phys. Lett.* **B727**, 417
- Nanova, M., *et al.* (CBELSA/TAPS) (2016), *Phys. Rev.* **C94** (2), 025205
- Nath, P., and R. L. Arnowitt (1981), *Phys. Rev.* **D23**, 473
- Nefkens, B. M. K., *et al.* (Crystal Ball) (2005a), *Phys. Rev.* **C72**, 035212
- Nefkens, B. M. K., *et al.* (Crystal Ball) (2005b), *Phys. Rev. Lett.* **94**, 041601
- Okubo, S. (1962), *Prog. Theor. Phys.* **27**, 949
- Okubo, S. (1963), *Phys. Lett.* **5**, 165
- Olbrich, L., M. Ztnyi, F. Giacosa, and D. H. Rischke (2018), *Phys. Rev.* **D97** (1), 014007
- Ottndad, K., and C. Urbach (ETM) (2018), *Phys. Rev.* **D97** (5), 054508
- Papenbrock, M., *et al.* (ANKE) (2014), *Phys. Lett.* **B734**, 333
- Patrignani, C., *et al.* (Particle Data Group) (2016), *Chin. Phys.* **C40** (10), 100001
- Peccei, R. D., and H. R. Quinn (1977), *Phys. Rev. Lett.* **38**, 1440
- Pena, M. T., H. Garcilazo, and D. O. Riska (2001), *Nucl. Phys.* **A683**, 322
- Pendlebury, J. M., *et al.* (2015), *Phys. Rev.* **D92** (9), 092003
- Petren, H., *et al.* (WASA) (2010), *Phys. Rev.* **C82**, 055206
- Pfeiffer, M., *et al.* (TAPS) (2004), *Phys. Rev. Lett.* **92**, 252001
- Pheron, F., *et al.* (Crystal Ball - TAPS) (2012), *Phys. Lett.* **B709**, 21
- Prakhov, S., *et al.* (A2) (2018), *Phys. Rev.* **C97** (6), 065203
- Rausmann, T., *et al.* (ANKE) (2009), *Phys. Rev.* **C80**, 017001
- Ringwald, A. (2015), PoS **NEUTEL2015**, 021
- Rodas, A., *et al.* (JPAC) (2017), *Phys. Rev. Lett.* **122**, 042002
- Roebig-Landau, M., *et al.* (TAPS) (1996), *Phys. Lett.* **B373**, 45
- Rosenberg, L. J. (2015), *Proc. Nat. Acad. Sci.* **112**, 12278
- Rosenzweig, C., J. Schechter, and C. G. Trahern (1980), *Phys. Rev.* **D21**, 3388
- Rosner, J. L. (1983), *Phys. Rev.* **D27**, 1101
- Rundel, O., M. Skurzok, O. Khreptak, and P. Moskal (WASA-at-COSY) (2017), *Acta Phys. Polon.* **B48**, 1807
- Sanghai, B., and Z.-p. Li (2001), *Eur. Phys. J.* **A11**, 217
- Saito, K., K. Tsushima, and A. W. Thomas (2007), *Prog. Part. Nucl. Phys.* **58**, 1
- Sakai, S., and D. Jido (2013), *Phys. Rev.* **C88** (6), 064906
- Schmidt-Wellenburg, P. (2016), arXiv:1607.06609 [hep-ex]
- Schroter, A., E. Berdermann, H. Geissel, A. Gillitzer, J. Homolka, P. Kienle, W. Konig, B. Povh, F. Schumacher, and H. Stroher (1994), *Z. Phys.* **A350**, 101
- Senderovich, I., *et al.* (CLAS) (2016), *Phys. Lett.* **B755**, 64
- Shifman, M. A. (1991), *Phys. Rept.* **209**, 341, [Usp. Fiz. Nauk157,561(1989)]
- Shimizu, H. (BGOegg) (2017), *Acta Phys. Polon.* **B48**, 1819
- Shore, G. M. (1998), arXiv:hep-ph/9812354 [hep-ph]
- Shore, G. M. (2006), *Nucl. Phys.* **B744**, 34
- Shore, G. M. (2008), *Lect. Notes Phys.* **737**, 235
- Shore, G. M., and G. Veneziano (1992), *Nucl. Phys.* **B381**, 3
- Shyam, R. (2007), *Phys. Rev.* **C75**, 055201
- Sigg, D., *et al.* (1996), *Nucl. Phys.* **A609**, 269, [Erratum: *Nucl. Phys.*A617,526(1997)]
- Skurzok, M., P. Moskal, N. G. Kelkar, S. Hirenzaki, H. Nagahiro, and N. Ikeno (2018), *Phys. Lett.* **B782**, 6
- Smyrski, J., *et al.* (COSY-11) (2000), *Phys. Lett.* **B474**, 182
- Smyrski, J., *et al.* (COSY-11) (2007), *Phys. Lett.* **B649**, 258
- Sun, W., L.-C. Gui, Y. Chen, M. Gong, C. Liu, Y.-B. Liu, Z. Liu, J.-P. Ma, and J.-B. Zhang (2017),



- arXiv:1702.08174 [hep-lat]
- Suzuki, K., *et al.* (2004), Phys. Rev. Lett. **92**, 072302
- Szczepaniak, A. P., M. Swat, A. R. Dzierba, and S. Teige (2003), Phys. Rev. Lett. **91**, 092002
- Tanaka, Y. K., *et al.* ( $\eta$ -PRiME/Super-FRS) (2016), Phys. Rev. Lett. **117** (20), 202501
- Tanaka, Y. K., *et al.* ( $\eta$ -PRiME/Super-FRS) (2017), Acta Phys. Polon. **B48**, 1813
- Tanaka, Y. K., *et al.* ( $\eta$ -PRiME/Super-FRS) (2018), Phys. Rev. **C97**, 015202
- Thomas, A. W. (1984), Adv. Nucl. Phys. **13**, 1
- Thomas, A. W., and W. Weise (2001), *The Structure of the Nucleon* (Berlin, Germany: Wiley-VCH)
- Thomas, C. E. (2007), JHEP **10**, 026
- Thompson, D. R., *et al.* (E852) (1997), Phys. Rev. Lett. **79**, 1630
- Toki, H., S. Hirenzaki, T. Yamazaki, and R. S. Hayano (1989), Nucl. Phys. **A501**, 653
- Tomiya, A., G. Cossu, S. Aoki, H. Fukaya, S. Hashimoto, T. Kaneko, and J. Noaki (2017), Phys. Rev. **D96** (3), 034509, [Addendum: Phys. Rev.D96,no.7,079902(2017)]
- Tsushima, K. (2000), Nucl. Phys. **A670**, 198
- Tsushima, K., D.-H. Lu, A. W. Thomas, and K. Saito (1998), Phys. Lett. **B443**, 26
- Urbach, C. (2017), EPJ Web Conf. **134**, 04004
- Vance, S. E., T. Csorgo, and D. Kharzeev (1998), Phys. Rev. Lett. **81**, 2205
- Veneziano, G. (1979), Nucl. Phys. **B159**, 213
- Vertesi, R., T. Csorgo, and J. Sziklai (2011), Phys. Rev. **C83**, 054903
- Waas, T., and W. Weise (1997), Nucl. Phys. **A625**, 287
- Weil, J., U. Mosel, and V. Metag (2013), Phys. Lett. **B723**, 120
- Weinberg, S. (1978), Phys. Rev. Lett. **40**, 223
- Weinberg, S. (1996), *The quantum theory of fields. Vol. 2: Modern applications* (Cambridge University Press)
- Wilczek, F. (1978), Phys. Rev. Lett. **40**, 279
- Wilkin, C. (2014), Acta Phys. Polon. **B45** (3), 603
- Wilkin, C. (2016), Acta Phys. Polon. **B47**, 249
- Wilkin, C. (2017), Eur. Phys. J. **A53** (6), 114
- Wilkin, C., *et al.* (ANKE) (2007), Phys. Lett. **B654**, 92
- Williams, M., *et al.* (CLAS) (2009), Phys. Rev. **C80**, 045213
- Willis, N., *et al.* (SPES3) (1997), Phys. Lett. **B406**, 14
- Witten, E. (1979a), Nucl. Phys. **B156**, 269
- Witten, E. (1979b), Nucl. Phys. **B149**, 285
- Witten, E. (1980), Annals Phys. **128**, 363
- Witthauer, L., *et al.* (A2) (2016), Phys. Rev. Lett. **117** (13), 132502
- Witthauer, L., *et al.* (A2) (2017), Phys. Rev. **C95** (5), 055201
- Wronska, A., *et al.* (ANKE) (2005), Eur. Phys. J. **A26**, 421
- Wycech, S., and W. Krzemień (2014), Acta Phys. Polon. **B45** (3), 745
- Xie, J.-J., W.-H. Liang, E. Oset, P. Moskal, M. Skurzok, and C. Wilkin (2017), Phys. Rev. **C95** (1), 015202
- Yamazaki, T., *et al.* (1996), Z. Phys. **A355**, 219
- Yorita, T., *et al.* (2000), Phys. Lett. **B476**, 226
- Zweig, G. (1964), CERN Report TH-412